Power System Risk Analysis Under Increasing Levels of Variable Energy Resources

Jacqueline Baum

A thesis
submitted in partial fulfillment of the
requirements for the degree of

Master of Science

University of Washington

2020

Committee:

Daniel Kirschen

Richard Christie

Brian Johnson

Program Authorized to Offer Degree:
Electrical and Computer Engineering

University of Washington

Abstract

Power System Risk Analysis Under Increasing Levels of Variable Energy Resources

Jacqueline Baum

Chair of the Supervisory Committee:
Daniel Kirschen
Electrical and Computer Engineering

As the portfolio of energy resources serving the electric power system transitions from a low to high percentage of stochastic energy resources, grid planners and operators must reevaluate the conventional methods used to characterize resource adequacy and the ability of power system generation sources to meet the modern electricity demand. This thesis reviews the historical and state-of-the-art methods used to evaluate resource adequacy, and presents a case study examining the reliability characteristics of a bulk power system with increasing wind and solar penetration (commonly referred to as variable energy resources). The scope of reliability in this thesis centers on probabilistic analysis of system resource adequacy. It provides examples of the pitfalls of misrepresenting dependencies in power generation from variable resources and proposes future work for further examination and extension of these concepts. A case study using historical weather patterns and correlated wind and solar generation in the WECC region of the U.S. is used to compare different reliability metric analysis methods. Results show that neglecting the generation uncertainty dependence model of variable energy resources significantly underestimates the risk of electric grid operation served primarily by variable energy resources; this highlights a major disconnect with the net load treatment of stochastic generation used prominently by system operators today. The accuracy of probabilistic models that represent system generation are of increasing importance in systems with high amounts of variable energy generation.

TABLE OF CONTENTS

LIST OF FIGURES

LIST OF TABLES

GLOSSARY

AGC: Automatic Generation Control

BPS: Bulk Power System

ELCC: Effective Load Carrying Capability

ENTSO-E: European Network of Transmission System Operators for Electricity

ERCOT: Electric Reliability Council of Texas

FOR: Forced Outage Rate

ISO: Independent System Operator

ISO-NE: ISO - New England

MISO: Midcontinent ISO

NERC: North American Electric Reliability Corporation

NREL: National Renewable Energy Laboratory

NWP: Numerical Weather Prediction

PJM: Pennsylvania-New Jersey-Maryland (Interconnection)

RTS-GMLC: Reliability Test System - Grid Modernization Laboratory Consortium

VER: Variable Energy Resource

WECC: Western Electricity Coordinating Council

WWSIS-2: Western Wind and Solar Integration Study, part 2

Chapter 1

INTRODUCTION

Methods for integrating high levels of renewable energy resources into the power grid are at a critical turning point in transitioning from thought experiments to reality. In the United States, municipalities and electric utilities have set deadlines as early as 2040 to transition their entire electric power portfolios to renewable energy. States including Washington, Wisconsin, California, Virginia, and New York have set goals of reaching 100% renewable electricity portfolios by 2050 [37]. While lawmakers strive to ensure that those new resource mix targets are met, electric utilities and ISOs are reevaluating their historical operational methodology to ensure that the new portfolio of energy resources can still meet the capacity needs of the system [25]. In 2019, state-by-state progress toward meeting their legislated renewable portfolio targets varied widely [38]; Figure 1.1 demonstrates the spread of annual electric generation mix by states with 100% renewable energy targets. A significantly different paradigm shift is posed to the electric grid operators in states like Wisconsin and Virginia, as compared to states like Maine and California which have already begun integrating significant portions of stochastic energy resources into their bulk generation mix. Consequentially, the probabilistic availability analysis of variable energy resources (VERs) like wind and solar is a central to this renewable energy transition.

1.1 Market Indicators of Reliability Concern

Governing regulators—such as NERC and ENTSO-E—mandate and enforce power balancing standards to ensure that system operators reliably deliver power to consumers. In order to meet these balancing standards and maintain grid stability, the system operator ensures

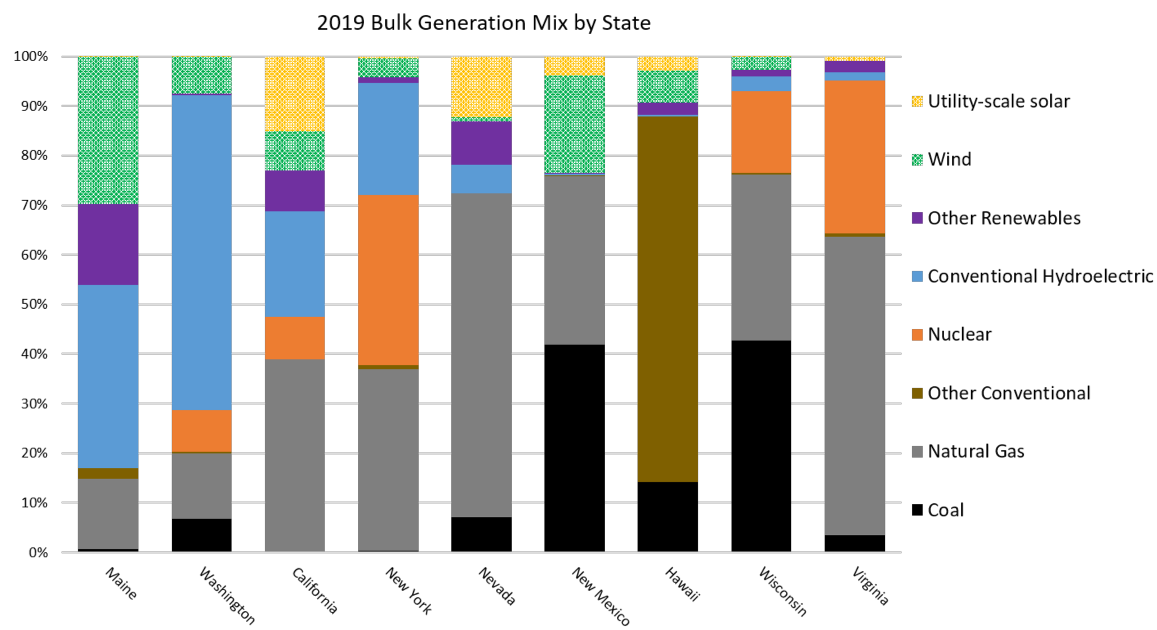

Figure 1.1: Total energy generation mix by state in 2019. All states shown have targets to reach 100% renewable energy by 2050. VERs (wind and utility-scale solar) shown in the patterned bar portion (adapted from [38]).

that electricity markets clear[1] with sufficient generating resources to continuously serve the forecasted load demand. This periodic demand forecast (hourly) includes small intra-period (five minute) load fluctuations and potential contingencies caused by large equipment outages. Rolling hourly forecasts horizons are typically 24 and 48 hours in advance, and five minute forecasts are typically made 4 hours and 1 hour in advance of real-time. The scheduled generators then provide enough power and reserve to maintain grid reliability and avoid cascading blackouts. Clearing the market to meet the reliability needs of the system requires a co-optimization of scheduled energy delivery and ancillary services. Following the approach of traditional, vertically integrated utilities, many energy markets were introduced with compulsory provision of frequency and voltage control for most generators intercon-

[1] Details on the electricity market clearing process and fundamentals of power system economics are covered in depth by [13].

necting and bidding into the market. Primary frequency control and basic voltage control were compulsory interconnect requirements in PJM as of 2007 [33]. Under this compulsory service structure, the system operator could take advantage of the standard droop curve and high inertia of conventional generators and use those voltage and frequency control services to manage power imbalances on the grid without necessarily compensating their service beyond energy delivery. As more stochastic generation resources enter the energy market, an increased need for ancillary services should galvanize an evolution in the economic incentives and general design of those services.

A stifling artifact of the conventional, compulsory method of acquiring ancillary services is that it wraps the cost of providing reliability services into the energy market. Rather than provide separate economic incentives for generators to reliably provide power, compulsory ancillary service interconnect requirements force all generators to incur their individual cost of providing the service capability without compensation for reliable dispatch. A generation resource pool with increased uncertainty (e.g. more stochastic generators) drives an increased need for reserve generation, and disproportionately pushes the cost of providing ancillary services to the dispatchable generators. This can increase the overall cost to the consumers because of the operational need to purchase excess reserve in order to provide the same amount of generation while maintaining reliability [33]. Further, without proper compensation (e.g. a call option) to provide the reliability service, the generator has inadequate incentive to deliver power reliably if called upon during an outage event. An ISO-NE Energy Security Improvements discussion paper aptly describes an example of these misaligned incentives [10]. From the energy supplier's perspective, the expected cost of acquiring adequate fuel reserves to deliver energy during a contingency event is higher than the expected remuneration for their participation. The case demonstrates a clear lack of economic incentive for unscheduled generators to bear the cost of maintaining fuel reserves despite the operator's expectation that the supplier will fulfill system interconnect requirements. This market design deficiency leaves the ISO at risk of failing to meet NERC's reliability and efficiency mandates; it increases the overall cost of supplying energy in an emergency situation and discourages generators from performing consistently.

In 2018, ISO-NE implemented Pay-for-Performance (PFP)[2] in an attempt to alleviate misaligned incentives and still meet regulatory mandates. The PFP market rule offers an incentive for generators to ensure their Capacity Supply Obligation (CSO) is satisfied during high load demand events. If a generator fails to meet its CSO during a "Performance Event", it incurs a charge based on the difference between the amount of supplied capacity and the Forward Capacity Market obligation. Similarly, the generator may receive a bonus payment for supplying additional power during the shortage event [9]. Under PFP rules, the generator could incur a staggering fee for failing to meet capacity expectations during a high demand event. However, if an unscheduled generator anticipates a low probability of being called upon during a Capacity Scarcity Condition, their expected penalization for underperforming will not outweigh the premium of purchasing advanced fuel reserves. ISO-NE expressed concern that despite the intentions of the PFP, the rule fails to properly incentivize generators to acquire adequate fuel reserves under realistic scarcity conditions [10]. The PFP rule is an insufficient economic driver because it only compensates or penalizes generator performance—it does not capture the ability to perform if called upon. This case emphasizes the value of ancillary markets in reducing supply and demand side risk. ISO-NE's new proposal of voluntary ancillary services includes a call option to cover the generator's cost of obtaining fuel reserves and reduces the system operator's risk of potentially failing to meet load demand [10]. As a voluntary service market, the design change also improves upon costly and technologically limiting restrictions of the compulsory ancillary service structure. System operators must critically evaluate new market incentives to adequately value availability in addition to performance in an effort to preserve reliability.

The challenge of designing and updating electrical energy markets to meet this changing resource portfolio extends well beyond ISO-NE. Part of MISO's short-term strategy for

---

[2]Pay-For-Performance began in 2018 and is being phased in over several years. By 2024, generators in the ISO-NE Forward Capacity Market will be responsible for a $5,455/MWh Capacity Performance Rate [9]

managing their changing grid is an enhancement of their Automated Generation Control for Fast Ramping resources. Starting in February of 2020, MISO altered their AGC system to allow for more resource agnostic participation while maintaining system reliability standards. Key components of the enhanced AGC program include a permissive charging mode[3] and an ancillary service clearing strategy that enables fast and slow responding resources to complement each other, rather than compete against each other. The upgrade also penalizes (and rewards) asset performance as a fast ramping device. MISO considers these regulation service upgrades essential to managing the uncertainty of their future renewable energy generation [19].

The authors in [7] examined the impact of revenue insufficiency, often termed the "missing money" problem, in ERCOT. With market structures at the time of the study, their research showed that generators face challenges in being adequately incentivized to invest in dispatchable capacity, particularly as the share of variable energy resources on the market grew. A lack of incentive for capacity expansion further strains the system's resource adequacy and reliability. ERCOT has more recently taken steps to augment their ancillary services market and address those revenue insufficiency issues. These changes come in response to increasing renewable production on the system, particularly from wind farms. One method that ERCOT has implemented is an "Under-generation Power Balance Penalty Curve" which applies a penalty price to generators for an overproduction or a shortfall of power capacity delivery. This penalty can also apply to the ramping capability of devices; five-minute up-ramp shortage prices can reach $9,000/MWh. This type of scarcity pricing intends to alleviate parts of the "missing money" problem faced by generators in energy markets with large amounts of low marginal cost producers. It "creates opportunities for resources that can respond to real-time shortages" with their fast ramping capabilities [29]. ERCOT has also revised their Ancillary Services product set to include new Fast Frequency Response reserve service and Contingency Reserve Service categories with the option for Load Resources to participate

[3]Permissive charging allows energy limited resources to recharge when the charging action helps return the system to a neutral operating condition.

in Under-frequency Reserve response. There are also performance-based awards for primary frequency response [6]. The combination of these additional market features clearly point to the need for grid operation mechanisms that can flexibly provide reliability to the changing mix of resources on the system.

1.2 Summary

The electricity market changes highlighted here underscore the relevance of ongoing research related to evaluating resource adequacy and reliability of power systems that are evolving to meet renewable energy production goals. Structural changes to ancillary markets indicate grid operators' concern about the mechanisms available for maintaining system reliability with high levels of variable energy resources in their generation mix. Grid operators not only need a way to respond to rapid fluctuations of power generation–they also need an appropriate measurement of uncertainty in the availability of generation resources. The probabilistic measurement of generation uncertainty and its use in reliability metric analysis is a fundamental part of managing this grid transition while maintaining reliability. As such, the present methods used to measure reliability must be reexamined for their fitness to evaluate bulk generation reliability with high VER penetration.

This thesis investigates the impact of various system assumptions when studying reliability metrics. It studies a collection of time-based reliability metrics under varied levels of renewable energy penetration and spatial correlation levels between renewable plants. Most importantly, it incorporates renewable capacity availability as a multi-state generating model based on the probabilistic forecast of power generation. This enables an analysis of the overall system risk with high levels of variable resources. The accuracy of such models is critical for both long-term system planning and reliable, short-term operations of day-ahead and real-time markets. An analysis is presented with data from the RTS-GMLC [1] and WWSIS-2 data from NREL [14].

Chapter 2

LITERATURE REVIEW ON RESOURCE ADEQUACY

2.1 Review of Reliability Metrics

This section provides background information on the topic of power system reliability, resource adequacy, and related information.

NERC's historical methodology recommendation for an ISO's assessment of resource adequacy is to evaluate the system's annual Loss of Load Probability (LOLP) against the system's peak load [21]. More recently, the Probabilistic Assessment Working Group at NERC has recommended that a collection of reliability metrics be applied to study resource adequacy [25]. No single metric comprehensively captures the magnitude, duration, and frequency of outage events, however an appropriate combination of reliability metrics can characterize the expected reliability of a region given its resource mix.

NERC and probabilistic reliability experts provide metric definitions as follows [22], where C_t is the capacity available at time t, and L_t is the load at time t:

- Loss of Load Probability (LOLP)
  - Probability of load demand exceeding available generation capacity at time t.

$$\mathrm{P}(C_t < L_t) = \sum_{c=0}^{C} \mathrm{P}(c = L_t), \text{ where } C = \min[C_{max}, L_t] \tag{2.1}$$

- Expected Unserved Energy (EUE)
  - Total expected energy loss (typically in MWh) over analysis period $[t_0, T]$.

$$\sum_{t=t_0}^{T} \mathrm{P}(C_t < L_t), \text{ where } t \text{ steps in hours} \tag{2.2}$$

- Normalized EUE (NEUE) gives a relative measure of EUE in parts per million. This can be useful for comparing regions with different magnitude load profiles.

- Loss of Load Event (LOLEv)
  - Count of load loss events, regardless of duration or magnitude of the event.

$$\sum_{t=t_0}^{T} \mathbb{1}[0 < \mathrm{P}(C_t < L_t)], \text{ where } t \text{ steps in hours} \tag{2.3}$$

- Loss of Load Expectation (LOLE)
  - Expected amount of time (e.g. hours, days, years) per analysis period that the available generation capacity will fail to meet load demand.

$$\sum_{t=t_0}^{T} \mathrm{E}[\mathrm{P}(C_t < L_t)], \text{ where } t \text{ steps in hours} \tag{2.4}$$

- Loss of Load Hours (LOLH)
  - Count of expected hours of lost load, regardless of the magnitude of loss.

$$\sum_{t=t_0}^{T} \mathbb{1}[0 < \mathrm{LOLE}], \text{ where } t \text{ steps in hours} \tag{2.5}$$

Reliability analysis experts emphasize the importance of comparing multiple metrics when evaluating the annual reliability of a system [17]. An example system, shown in Table 2.1, highlights how a single metric comparison can misrepresent the overall reliability of a system. In each scenario, the system under analysis experiences identical total EUE, but the number of LOLEv's and period-by-period metrics show drastically different day-to-day or hour-to-hour power and energy delivery to customers. The cases require a system operator to commit very different generation profiles of capacity and flexibility in order to meet the system needs. For example, avoiding frequent but small magnitude outages, like in Case 3, requires operators to commit more long duration and low capacity resources. Avoiding an outage scenario in Case 1, contrastingly, requires a short duration and high capacity resource addition. Yet if the system was designed to meet only 1 standard (EUE or LOLEv), the reliability analysis would inadequately characterize the system's needs.

Table 2.1: Reliability metric comparison, adapted from [17]

	Case 1		**Case 2**		**Case 3**	
Period	EUE	LOLEv	EUE	LOLEv	EUE	LOLEv
1			20	1	10	1
2					10	1
3			20	1	10	1
4			20	1	10	1
5					10	1
6					10	1
7			20	1	10	1
8	100	1			10	1
9			20	1	10	1
10					10	1
Total	**100**	**1**	**100**	**5**	**100**	**10**

Milligan notes that a combination of these metrics can extend the understanding and characterization of system reliability [17]. For example, $\frac{\text{LOLH}}{\text{LOLEv}}$ gives the average length of loss of load events; $\frac{\text{EUE}}{\text{LOLEv}}$ gives the average energy lost during a loss of load event. Regardless of the metric of choice, it's challenging to directly quantify the accuracy of these system reliability metric predictions because a potential outage event (i.e. high LOLP scenario) will typically be avoided through precautionary system correction. However, the underlying VER output model forecast accuracy can be evaluated with methods described in [30].

As the technical characteristics of generation resources serving the grid evolves (e.g. flexibility for ramping, duration of power availability), a rigorous evaluation of the reliability impact of the system's generating capacity mix is critical. For example, the impact of adding a new solar plant compared to an energy storage facility influences metrics such as EUE and LOLH differently. These relationships will be examined in Section 3.1.

2.2 Methods for calculating System Generating Capacity

A variety of metrics are valuable for evaluating power system reliability, but the probability of system capacity availability (or, complementary, the capacity outage probability) is central to the calculation of all the reliability metrics mentioned in Section 2.1. This section describes common methodologies used to calculate the system capacity outage probability and emphasizes the importance of accurately capturing the spatio-temporal correlations associated with integrating variable energy resources into the bulk power system.

2.2.1 Classic Methodology: Recursive Convolution of System Capacity Availability

The fundamental method for calculating the Capacity Outage Probability is described in [4]. This system outage probability represents the likelihood that generating capacity C_i will be unavailable to the system given the joint probability of N individual generators $g_1, g_2, ..., g_N$ having unexpected outages totaling C_i. The textbook method represents this probability as a discrete distribution. The sum of independent random variables can be calculated through convolution. In this case, the sum represents the total capacity outage (or total capacity availability), and the probability density function given by the convolution of individual generator Forced Outage Rates (FORs) returns the Capacity Outage Probability of the system. The characteristic of independence between power generation units enables the use of convolution because the joint distribution of generation can be replaced with the marginal probability distributions of each individual generator [35]. This independence characteristic enables the capacity outage probability (or capacity availability probability) of the system to be calculated in a recursive manner using the method provided in [4].

Neglecting transmission constraints, the joint capacity availability of a system with N generators $g_1, g_2, ..., g_N$ with corresponding discrete availability distributions $f_1, f_2, ..., f_N$ can be found by recursively convolving the capacity availability of each generator into the total system capacity [42]:

$$f_{\alpha+\beta}(C_i) = \sum_{j=C_{i_{min}}}^{C_{i_{max}}} f_\alpha(j) f_\beta(C_i - j), C_i \in [g_{\underline{\alpha}} + g_{\underline{\beta}}, g_{\overline{\alpha}} + g_{\overline{\beta}}] \tag{2.6}$$

Equation 2.6 is initialized with generators g_1 and g_2 and repeated through g_N, giving the complete system capacity availability $f_{g_1+g_2+\ldots+g_N}(C_i)$.

The following examples demonstrate characteristics of these capacity availability probability distributions which will be applied to case studies in Section 3.1.

Example of Independent Generators with varied availability

In this basic example, 30 generic generators rated at 50MW with identical availability rates λ are convolved to assess their joint probability of capacity availability. As the uncertainty of generation increases (i.e. availability rates decrease), the joint capacity availability curve exhibits a wider probability spread. As uncertainty of availability is reduced, the curve steepens. This relationship is demonstrated in Figure 2.1.

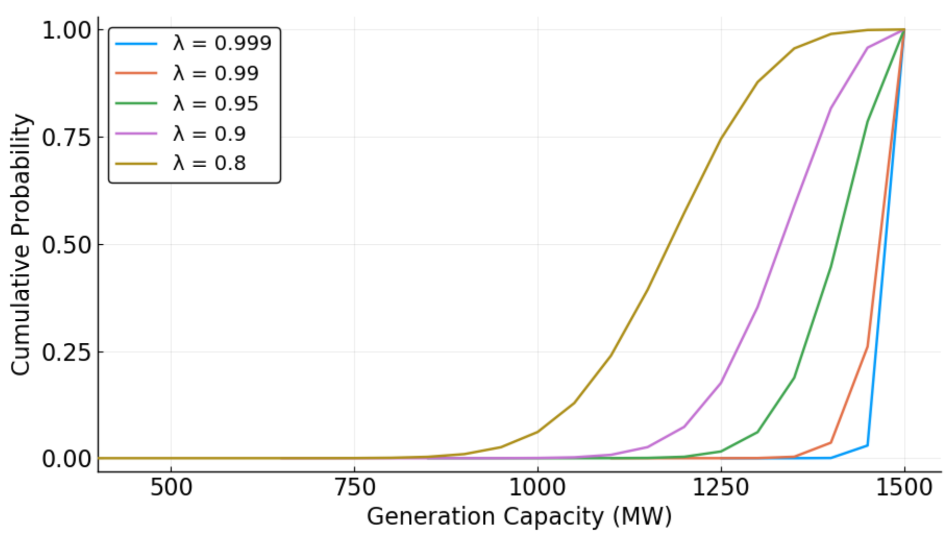

Figure 2.1: Joint capacity of (30) 50MW independent generators at varied levels of availability. Trends represent availability rates λ ranging from 85% - 99.9%.

In power systems with primarily conventional energy resources, the spread of the availability curve remains relatively constant over time[1], indicating that the reliability risk of an X MWh EUE is equivalent across all points in time. However, the relative risk of X MWh EUE varies based on the spread of the capacity availability curve. Following the example shown in Figure 2.1, the relative risk of an outage in a system with availability $\lambda = 0.85$ is lower than the relative risk in a system with availability $\lambda = 0.99$ because an incremental load increase results in a higher MWh EUE on the system with a steeper availability curve. The concept of using reliability metrics as an indicator of real-time risk is explored in [12].

For systems with uncurtailed, low levels of VERs, the capacity availability of the VERs are often treated as a net load [22] [32]. This methodology is straightforward, where the net load N_t at time t,

$$N_t = \sum L_t - \sum \mathrm{VER}_t \tag{2.7}$$

for load L_t and total variable resource output VER_t.

By treating renewable generation as a simple load reduction, the contribution of VER is only approximately included in a classic reliability index calculation because the VER output at any time t strictly shifts the capacity availability curve in one dimension along the capacity axis.

While the net load and VER assumption enables computational convenience, the accuracy of this assumption should be examined as proportions of VER grow.

Example of COPT on RTS-GMLC

An example of the cumulative distribution of capacity availability is shown in Figure 2.2. This distribution is effectively the complement to the classic Capacity Outage Probability Table from [4], where a point on the shown curve represents the probability that the system capacity will be below x MW. In traditional loss of load probability analysis, the load is

[1] FORs do change seasonally, but they are constant relative to the temporal rate of capacity availability change for VER.

subtracted from this capacity availability curve, effectively shifting the curve to the left along the x-axis. Figure 2.2 shows an example of the capacity curve net load, with a typical mix of conventional, independent generators with 2-state outage rates.

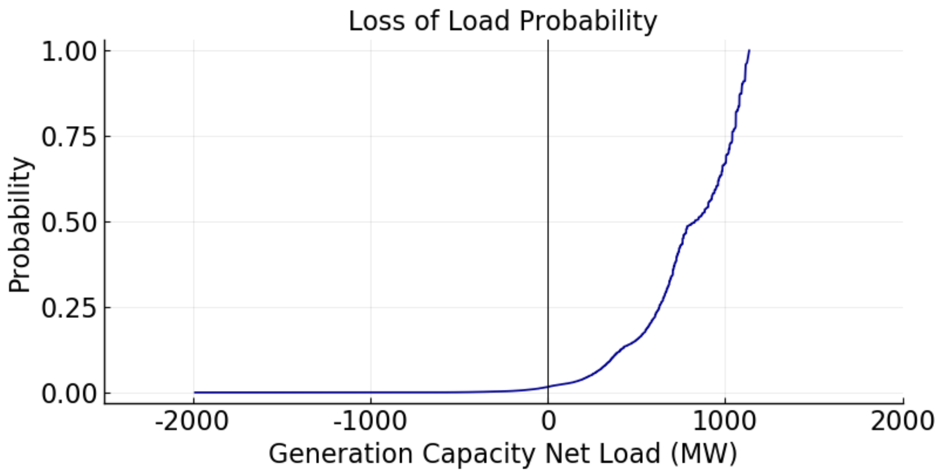

Figure 2.2: Loss of load probability distribution (generation capacity net load) example of the conventional generation from the IEEE RTS-GMLC data set. Sample taken from system load on July 26 at 21:00.

While it is common to use a simple 2-state FOR to calculate the availability of conventional generation, the recursive convolution method is not limited by 2-state availability models. Using the recursive convolution method from Equation 2.6, the LOLP at any point in time is found by subtracting the load from the capacity availability distribution (as shown in Equation 2.1).

2.2.2 Adaptations of System Generating Capacity Probability

Incorporating variable energy resources into the calculation of capacity availability presents a unique challenge because of the spatial and temporal dependencies that constrain the intermittent resource outputs. Defining a rigorous and tractable method to calculate the probability of capacity availability for a system with mixed independent, conventional generation and variable energy resources is an active area of research [24] [2]. The prominent techniques for capturing the capacity availability of systems with VER are discussed in this section.

Transformation of Point Forecasts to Density Forecasts

The capacity availability of individual VERs is inherently captured in the generation density forecast of each VER. The topic of forecasting variable resource outputs is beyond the scope of this thesis, but the distinction between point forecasts and density forecasts is key to this area of research. A density forecast is a probability distribution that describes the likelihood of all event scenarios; a point forecast is a single value that describes the expected outcome of an event. When using historical data to calculate the capacity availability of VER, it is common that only the time-series point forecast data will be accessible. In this case, the point forecast must be transformed into a density forecast before further analysis on capacity availability can be completed. For a more rigorous analysis, the original density forecast used by the system operator should be applied. Pinson provides a VER adapted method for transforming existing point forecasts into density forecasts [30]. The method is an extension of statistical bootstrapping, where historical error samples ϵ are transformed into a density forecast based on confidence intervals of the error probability. The error samples are found from the historical data $\epsilon = y - \hat{y}$, where y and $\hat{y}$ are the time-aligned actual outputs and forecast outputs respectively. Using this method, the point forecast at each time t is transformed into a distribution of outputs and corresponding probabilities.

After the density forecasts of VER are obtained, it is tempting to consider the capacity distributions as conventional generators and convolve the distributions recursively into the overall system capacity availability distribution (as in Equation 2.6). While this appears computationally convenient on the surface, consideration must be given to the correlation and dependencies between each VER capacity availability.

Capturing Correlation

Spatial and temporal correlations between the outputs of solar and wind plants have been studied extensively [24] [8] [31] [34] [15] [40].

A simple test for this correlation can be executed by computing the rank correlation between the historical outputs of variable energy resources. The rank correlation is used in preference to the product moment correlation because it better expresses the dependence structure of non-Gaussian distributions [26].

In [27], Papaefthymiou and Kurowicka demonstrate significant correlation between spatially diverse renewable plant output forecasts. Their research asserts that even across large geographic distances, the effects of uncertainty correlation are present. Most importantly, they demonstrate the significant error that results from modeling renewable resources as independent generators rather than dependent sources of power. They present a foundational method for modeling this dependence using Sklar's theorem and copula functions to link renewable generators. Papaefthymiou and Pinson similarly provide evidence for the importance of accurately modeling renewable dependence in [28]; the authors model spatial dependence in wind forecasts and produce similar results.

A model of statistically dependent time-varying outputs is examined by Borges and Dias in [5] to capture the influence of different dependence assumptions on reliability metric calculations. The results emphasize that inaccurate capacity availability modeling at low renewable penetration is masked by the higher portion of independent, conventional generation sources. At high renewable penetration levels, the independent capacity availability model falsely appears to have much better reliability than the statistically dependent model of resource generation.

The impact of correlation between wind regions on calculating LOLP and EUE is examined by Tomasson and Soder in [36]. The authors found similar results to Papaefthymiou and Pinson [28], indicating that wind output correlation is statistically significant, even with large spatial diversity. In their study of Denmark–with wind farms and weather forecast regions spanning $43,000$ km^2–even the furthest regions regions exhibited an average rank correlation over 0.3 at a 24-hour look ahead forecast.

Mathematically, the joint probability of two or more random variables can only be represented by the product of their marginal probability distributions if the random variables are independent [35]. Given the extensive evidence of nonzero correlation between generation profiles of VER, the application of recursive convolution is not a valid method for calculating the joint probability of total VER generation. VER forecasts are dependent and should be treated that way when being incorporated into capacity availability models. In other words, the joint distribution of total VER output forecast is required to find the accurate probability distribution of total system capacity availability.

Copula Theory

Obtaining the joint distribution of dependent random variables has been studied extensively in probability theory [20]. Copula theory can be applied to define the relationship between unknown joint or marginal distributions. According to Sklar's theorem, the joint CDF $H(X,Y)$ of any two dependent functions $G(X)$ and $F(Y)$ can be represented through a unique copula function C:

$$H(X,Y) = C(F(X), G(Y)) \tag{2.8}$$

The joint probability density function $h(x,y)$ can similarly be represented through the copula density function:

$$h(x,y) = c(F(X), G(Y))f(x)g(y) \tag{2.9}$$

This theory extends to the joint pdf of any n marginal, dependent pdfs:

$$h(x_1, x_2, ..., x_n) = c(F_1(X_1), F_2(X_2), ..., F_n(X_n))f_1(x_1)f_2(x_2)...f_n(x_n) \tag{2.10}$$

where h represents the joint distribution of the random variables $X_1...X_n$. A detailed introduction to the study of copula functions is provided by Nelsen in [20].

Copula theory can be applied to study the joint distribution between VER capacity availability when only the marginal distributions (i.e. density forecasts) of capacity availability are known. The copula function, commonly referred to as a copula, links the dependencies of the marginal distributions; the resulting joint distribution can then be appropriately convolved with the independent generator capacity availability distributions to obtain a complete system capacity availability distribution.

Sklar's theorem shows that a copula can be used to represent the joint distribution of any two functions, however, the selection of an appropriate copula presents mathematical challenges. In the case of representing the output of variable energy resources, the non-parametric, asymmetrical nature of joint VER capacity availability unfortunately limits the use of common copulas, like the widely prevalent Gaussian distribution and normal density copula. The applicability of the Gaussian copula relies on the underlying marginal distributions having symmetrical joint dependencies. Archemedian copulas have asymmetrical properties that are better suited for representing the joint dependencies of variable resource output distributions without losing the dependence characteristics at the tail ends of the distributions.

The application of copulas to wind power models is investigated in further detail by Louie in [16]. In particular, it is found that while the use of Gaussian copula functions is convenient for multivariate distribution modeling, statistical testing shows that a Gaussian model fails to adequately capture the dependence characteristics of wind outputs. Louie provides a reference table for appropriate copula selection based on the rank correlation of the system under study. The Gumbel copula family appears to be most widely applicable, however the author cautions that variations may exist for site specific circumstances, and that statistical tests should be applied to evaluate the best copula for reliability analysis and other studies. Papaefthymiou also provides guidance on evaluating the fitness of specific copulas to data for wind systems in [26].

Dependent Discrete Convolution

Given the importance of accurately capturing dependence in joint probability models, the next challenge is including those models in the system joint capacity availability formulation. This is a necessary input to the calculation of various reliability indices. The Dependent Discrete Convolution method is generalized by Zhang et al. in [42], which intends to address this issue. The authors provide a mathematical formulation of the convolution necessary to calculate a system capacity availability while maintaining the dependence between generation resource uncertainty.

One clear limitation of the formulation in [42] is the two-variable factor–the derivation for Dependent Discrete Convolution given in [42] only extends to 2 dependent generation sources. In a power system with tens or hundreds of dependent variable generation plants, an efficient multivariate dependent discrete convolution method is necessary. In [41], Wang et al. provide a generalized method for N variables. As the authors note, this problem quickly encounters the curse of dimensionality. With N dependent variable resources modeled and each model containing K discrete steps, the computational complexity is K^N. In [41], the authors propose a method to reduce the complexity of the problem by creating subgroups of the N variable resources based on their correlation structure. A threshold of dependence is used to then treat each subgroup as an independent generation resource. Then, the independent subgroups can be more quickly convolved into an overall joint availability distribution using the classic recursive method for evaluating system generation availability. There are trade-offs between computational speed and model accuracy when determining the appropriate dependence threshold as well as the number of discrete steps K to use in representing the marginal capacity distribution of each renewable generation plant.

2.3 Applications and Analysis of Metrics in Literature

In 1992, Billinton et. al. proposed methods for incorporating renewable resources in system reliability and resource adequacy, particularly for wind energy [3]. The study provides a basic method for combining the capacity of Wind Energy Conversion Systems (WECS) with conventional generating capacity resource adequacy assessments. It includes a multi-state capacity availability approach for wind power plants and compares the expected unserved energy metric with the "classic" method of considering renewables as net load. The results of the paper primarily show that adding system capacity increases system reliability.

In [12], Kirschen et al. contend that real-time security assessments should be approached probabilistically instead of deterministically. There is an emphasis on the need for a continuous risk measurement that can be calculated during real-time operations. This is particularly important for low probability contingencies with high potential for damage. The paper seeks to provide a measure of the probability of involuntary load disconnects necessary to improve system security. It computes a linear reference scale of expected unserved energy then uses the scale for faster computation and comparison of relative risk during real-time operations. Using a linear indicator is valuable because it can better warn system operators about worsening conditions. The load to available generation capacity ratio of the system is a non-linear indication of system stress. If an operator was focused primarily on system loading conditions, it would be very difficult to discriminate between an extremely high risk and lower risk scenario—small changes to loading suddenly have severe changes to outage probabilities. Alternatively, by using a relative, linear scale that indicates real-time risk, operators can take more informed action as system conditions worsen.

Extensive studies on increasing renewable energy resource integration have been completed [14]. Phase 2 of the Western Wind and Solar Integration Study (WWSIS-2) investigates the build-out of a significant amount of wind and solar generation in the Western Energy Interconnect. Interested readers are encouraged to review the results of the study in detail, but a couple of key modeling decisions influenced the research in this paper. First, the authors use historical solar and wind data from Western U.S. system operators, plus detailed Numerical Weather Prediction (NWP) models and advanced data synthesis tools. The error distributions of the VER forecasts spanning various look-ahead timescales were examined by Hodge and Milligan in [8] and incorporated into the day-ahead and 4-hour-ahead forecast models used in the WWSIS-2. Dependency between individual wind and solar generation sites was captured implicitly through the NWP used to create their production forecasts. In the study's scheduling model, the hourly system reserves were set to compensate forecast errors at 95% confidence intervals.

A summary of strategies applied to evaluating the risk of cascading outages is provided by the IEEE PES Task Force on Understanding, Prediction, Mitigation, and Restoration of Cascading Failures and in [39]. The authors evaluate various risk assessment methods and tools on their accuracy, computation speed, and adaptability to new test scenarios. A weakness identified in the general "Probabilistic Simulation" approach is the trade-off made between modeling approximation and simulation speed. Selecting an assessment methodology with appropriate level of detail for the intended application was highlighted as important.

Pinson et al. utilize their model of dependence between wind generation plants to optimize bidding strategies for wind farms in [31]. In this case, the dependence model informs the generation bid strategy for each wind farm to minimize revenue losses, particularly weighting shortage penalizations.

An exploration of research on resource adequacy and reliability metrics is discussed by Milligan in [17]. The industry need to focus on "energy first" planning is emphasized, meaning that system operators should focus on taking full advantage of the energy provided by variable resources (e.g. wind and solar), then fill in the uncertainty gaps with fast-dispatchable resources. This is counter to the historical focus on peak-load-centered capacity planning. Resource planning in the past has heavily focused on planning reserve margins, which Milligan cautions are becoming ever more useless with growing variable energy penetrations. The problem with using calculated planning reserve margins is that they focus on peak system demand which doesn't necessarily align with periods of high uncertainty from variable resources. If the reserve is planned on peak demand, the probability of failing to have enough reserves to compensate for generation variability increases.

The importance of increasing the time step resolution of probabilistic reliability analysis to more accurately capture the loss of load probability when higher levels of VER are used to meet load demand is examined by Milligan et al. in [18]. The "diminishing returns" on the Effective Load Carrying Capability (ELCC) of VER capacity as it delivers a higher percentage of the peak load is highlighted. The paper also includes a discussion on the ELCC "shifting" the load carrying capacity of the system. The authors also offer evidence of significant differences between ELCCs based on their method of calculation. Approximation accuracy can vary significantly based on the selection of peak load hours and other factors. The importance of using multiple years worth of historical data is also emphasized; this is because the ELCC needs to capture the seasonal and annual weather pattern changes that impact electricity demand and are correlated with renewable production—particularly wind power. However, multi-year data can also contain demand changes driven by economic or other factors that are uncorrelated with VER production.

2.4 Summary

A vast amount of research exists on the topic of resource adequacy and reliability metrics for bulk power system analysis. Methods for quantifying the real-time operational reliability impact of variable energy resources do exist, however the application of mathematically rigorous probabilistic analysis methods is limited. As the capacity of VER on the grid continues to grow, researchers should critically examine the method(s) applied to evaluate power system reliability.

Chapter 3
RELIABILITY CASE STUDY

A combination of point forecast transformation, discrete dependent convolution, and empirical estimation are used to calculate the joint capacity availability probability of spatio-temporally correlated VERs (as described in Section 2.2.2). These methods were selected as a combination of a state-of-the-art approach (discrete dependent convolution) with a computationally tractable approach (empirical estimation). This adapted method is applied to a test system to evaluate the impact of neglecting VER correlation in capacity availability models on reliability metrics. The joint capacity availability model is considered under varied spatial regions and VER penetration levels. The resulting reliability metrics are compared with reliability metrics calculated using conventional capacity availability assumptions.

3.1 Test System Description

The study represented here uses the Reliability Test System Grid Modernization Lab Consortium (RTS-GMLC) data set; this power system data is a modernized version of the classic IEEE Reliability Test System [1]. The variable energy resource data in the RTS-GMLC is based geographically and temporally on a roughly 250x250 mile region in the Southwestern United States. Additional wind and solar data from the WWSIS-2 database [14] was added to the system to study wider geographic diversity while maintaining correlated temporal and weather patterns. Transmission parameters and constraints are defined in the RTS-GMLC, however, a copperplate model[1] is assumed here to isolate the reliability impact of correlated VER production uncertainty from the impact of transmission constraints and potential for

[1]Copperplate transmission models assume economic dispatch of generation resources and no overloading of transmission lines. Research on modeling and addressing transmission constraints is explored in [11] and [14].

cascading outages from sympathetic protection tripping.

A joint probability model of the total VER output is generated by the following process:

1. Apply a joint density estimation to the historical VER forecast distributions[2].

2. Condition the joint probability distribution to the density forecast of VER production.

3. Convolve the statistically estimated, joint conditional probability model of VER capacity availability with the independent capacity availability model of the conventional generation resources in the test system.

The resulting correlated system capacity availability model is referred to as the "Joint" model in the remainder of this section.

Two probability models based on the assumption of independent VER generation were created as comparisons to the Joint model. These models follow the classic "net VER" convolution method described in [32]. In this approach, only independent, conventional generation is considered in the capacity availability probability model, and the time series wind and solar generation are subtracted from the load profile at each time step t. The first "net VER" model is created using the day-ahead wind and solar forecasts at time t; the second "net VER" model is created using the actual wind and solar production at time t. These models are respectively referred to as the "Day-Ahead Forecast" and "Perfect Forecast" models in the remainder of the thesis. Although the "net VER" model may appear to be an overly simplistic alternative to the Joint model, its pervasive use in both industry and state-of-the-art research justifies its application for this study[3].

---

[2]Totalized wind and solar curves are generated using nonparametric frequency estimation to avoid misrepresenting the resource behavior from an application of a generic probability distribution that fails to capture the actual dependencies of the system. This gives the modeling process used here more flexibility for applications to other systems which may have different underlying probabilistic characteristics.

[3]Borges and Dias include a comparison of independent VER and joint VER probability distributions in a similar study [5]. Their results indicate that the independent VER models produce reliability metrics with an order of magnitude higher error than the joint model and require double the computational time.

All three discrete, nonparametric capacity availability probability distributions (Joint, Day-Ahead Forecast, and Perfect Forecast) are evaluated over 1 full year of new VER production data. Hourly LOLP and EUE are calculated for each model with PRAS[4] using the temporally aligned load, wind, and solar production data from the test system. Additional reliability metrics were generated from the hourly LOLP and EUE data using equations from Section 2.1. Statistical measures of skewness and kurtosis of the resulting distributions are also calculated to compare the characteristics of the three models.

3.2 Test Scenarios, Results, and Discussion

3.2.1 Scenario Overview

Using the data and capacity availability models from the system described in section 3.1, 15 subsets of the system generation data were selected to evaluate and compare reliability metrics calculated with the Joint, Day-Ahead, and Perfect Forecast models. The 15 subset scenarios represent Low, Medium, and High VER penetration levels across 5 nested geographic regions. The increasingly larger geographic regions act as a control for differing levels of spatial correlation between VER in the system; as noted in 2.2.2, smaller geographic regions tend to have higher VER correlation. The nested geographic regions used to test spatial correlation are shown in Figure 3.1. Details on the locations of individual solar and wind generation locations are shown in Figure A.1 in Appendix A.

[4]Probability Resource Adequacy Suite, an open-source reliability analysis tool from NREL [23]

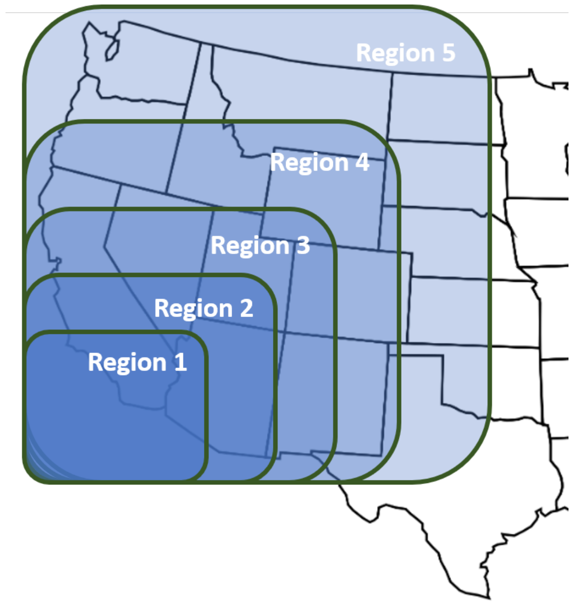

Figure 3.1: Approximate geographic locations used to select VER resources for each region in the spatial correlation study.

Total nameplate capacities by resource type selected for each test scenario are shown in Figure 3.2; details are provided in Tables A.1−A.3 in Appendix A. The "Conventional" resource category consists of:

- (1) 400MW nuclear plant; FOR = 0.12
- (#) 50MW generic generators[5]; FOR = 0.02

[5]An adjusted number of generic, dispatchable generators are used in the model to maintain a consistent load to generation capacity ratio and present comparable availability of the resource. Extended discussion on this model choice is covered in Section 4.1.1

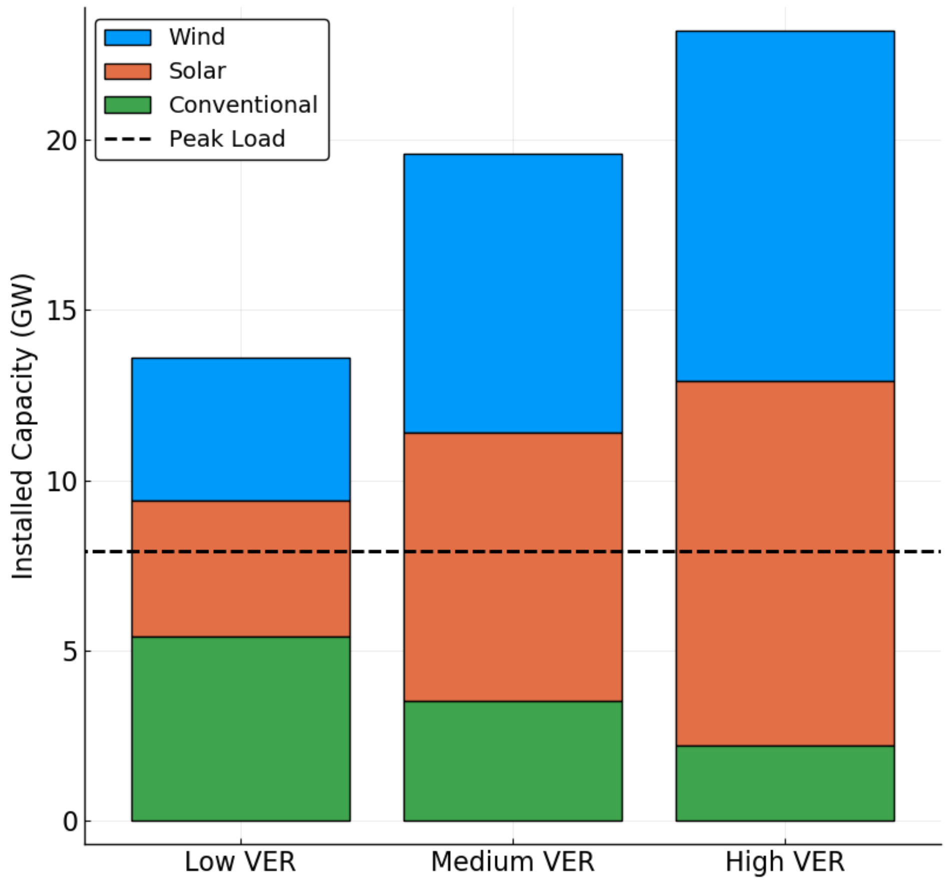

Figure 3.2: Proportions of installed capacity by resource type for Low, Medium, and High VER scenario studies. Peak system load shown for reference.

Computation Information

The system model was built in the programming language Julia version 1.3 and ran on a machine with an i7 CPU with 16GB of RAM. A complete reliability metric analysis run for 1 of the 15 subset systems (e.g. Medium VER in Region 2) required between 43 - 67 seconds to execute.

3.2.2 Results

Impact of VER proportion and spatial correlation

The resulting reliability metrics from each scenario evaluation exhibit a few trends. Regardless of the underlying capacity availability model, the calculated reliability metrics worsen with increased VER level in every scenario. This is evident from the annual LOLE and EUE reliability metrics calculated for each scenario, shown in Tables 3.1−3.6. Despite the perhaps obvious simplifications behind the net VER models, the order of magnitude difference between the net VER reliability metrics and the Joint model metrics is noteworthy. Additionally, increasing the spatial region of the selected wind and solar generation sites (i.e. moving from sub-systems in Region 1 to Region 5) showed improved reliability metrics for all underlying capacity models. This indicates that increasing the geographic diversity of VERs can improve system reliability. However, the return on reliability improvement diminishes at spatial Region 3 and beyond. These trends support previous research (as highlighted in section 2.3) showing that spatio-temporal correlation and VER availability modeling both play a critical role in power system reliability analysis. A sample of the Loss of Load Probability distributions for a single hourly period is shown in Figure 3.3.

A few characteristics of the resulting LOLP distributions are noteworthy. The spread of the Joint model is clearly much wider than that of the Perfect and Day-Ahead VER models; this results in the significantly higher EUE and LOLE metrics seen by the Joint model because the tail of the distribution crosses the 0 MW available capacity threshold more frequently. The time snapshot shown in Figure 3.3 highlights a common case where the aggregate VER forecast differs from the actual aggregate VER output; the Day-Ahead VER Forecast model sees nearly 0% LOLP, but perfect foresight indicates that the net VER LOLP is over 10% (a concerning amount compared to average, reliable conditions). The Joint VER model manages to capture the uncertainty of VER production through the wider spread of its distribution at this moment in time.

Using temporally aligned VER output profiles and load profiles to conduct the reliability

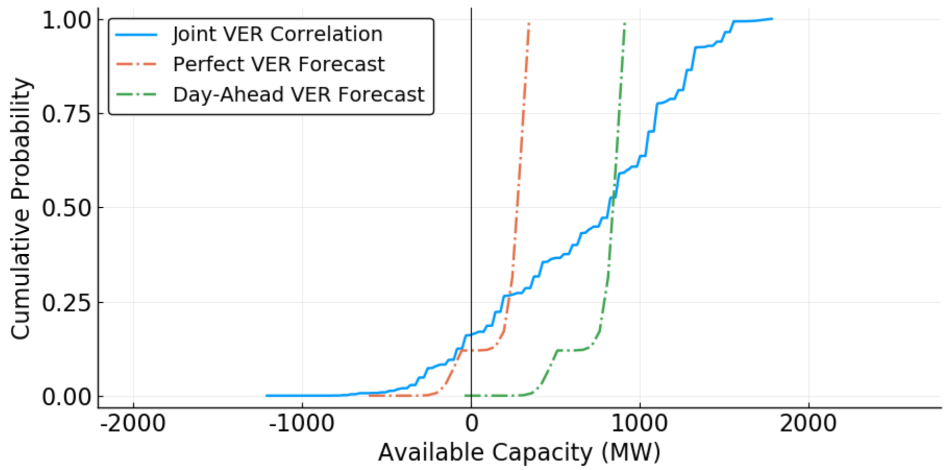

Figure 3.3: Loss of Load Probability snapshot during a July night from Region 5, High VER system. The 0MW axis crossing indicates the LOLP of each model distribution at the sampled t step.

metric analysis provides valuable insight into the temporal frequency of outage events. Figure 3.4 highlights why the conventional notion that credible loss of load events only occur during peak load conditions must evolve. As the proportion of VERs serving system load grows, so does the likelihood that load loss events occur during medium and light system load conditions.

Impact of underlying reliability model

The resulting reliability metrics from each capacity availability model (Joint, Day-Ahead Forecast, Perfect Forecast) capture important information for future modeling. A failure to account for spatial correlation of totalized VER forecast errors drastically underestimates the loss of load probability, particularly in tightly spatially coupled regions.

The gap in calculated reliability metrics between the joint model and the “net VER” models reduces as the spatial region increases. This again indicates that the spatial correlation of forecast errors and total capacity availability is more important when analyzing smaller regions supplied by VER. Sample plots of the resulting Loss of Load Probability dis-

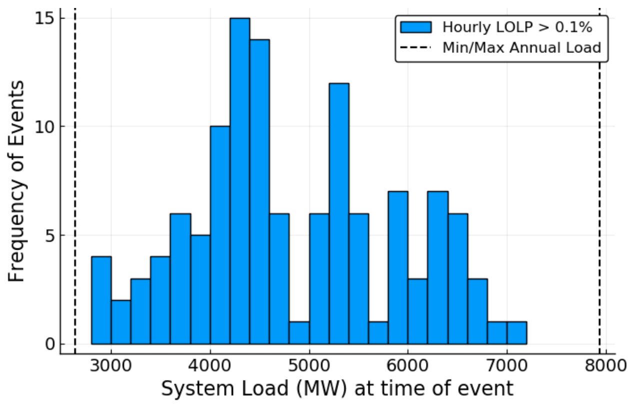

(a) High VER, Region 1

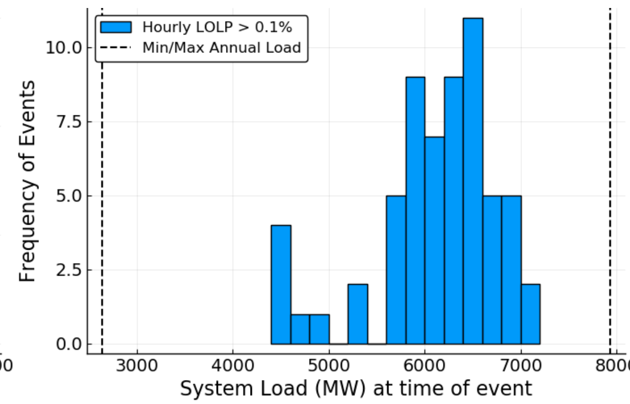

(b) High VER, Region 5

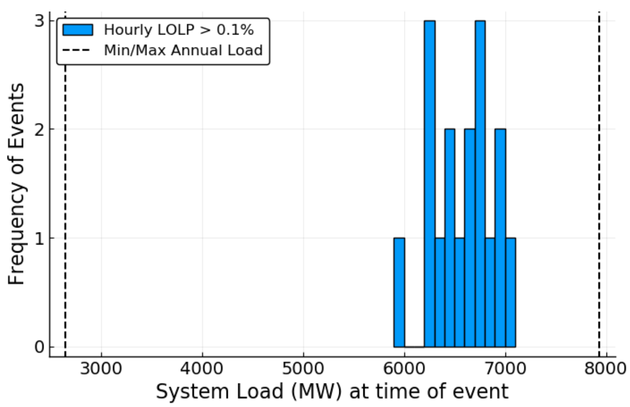

(c) Low VER, Region 1

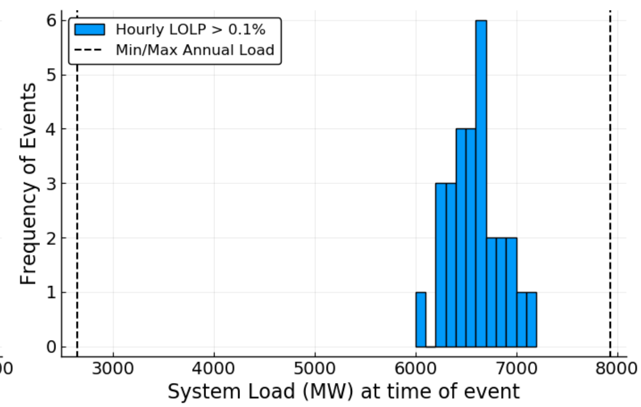

(d) Low VER, Region 5

Figure 3.4: Histogram of events where (LOLP > 0.001) at respective hourly system load.

tributions (cumulative availability net load) for the models are shown in figures 3.5 and 3.3. Appendix A shows additional plots. When reviewing the resulting LOLP curves, the simplicity of the Net VER models is clear. The shape of the Net VER model (its skewness and kurtosis) remains constant and shifts along the x-axis as the VER output and load changes. Thus, the Perfect VER and Day-Ahead VER models always have the same shape. The Joint VER model, on the other hand, clearly changes its shape at each instant in time (due to the changing VER availability at the given instant). The spread of uncertainty captured by the Joint model also spans a wider range of potential capacity outputs (i.e. the distribution support) because of the multi-state VER availability distribution.

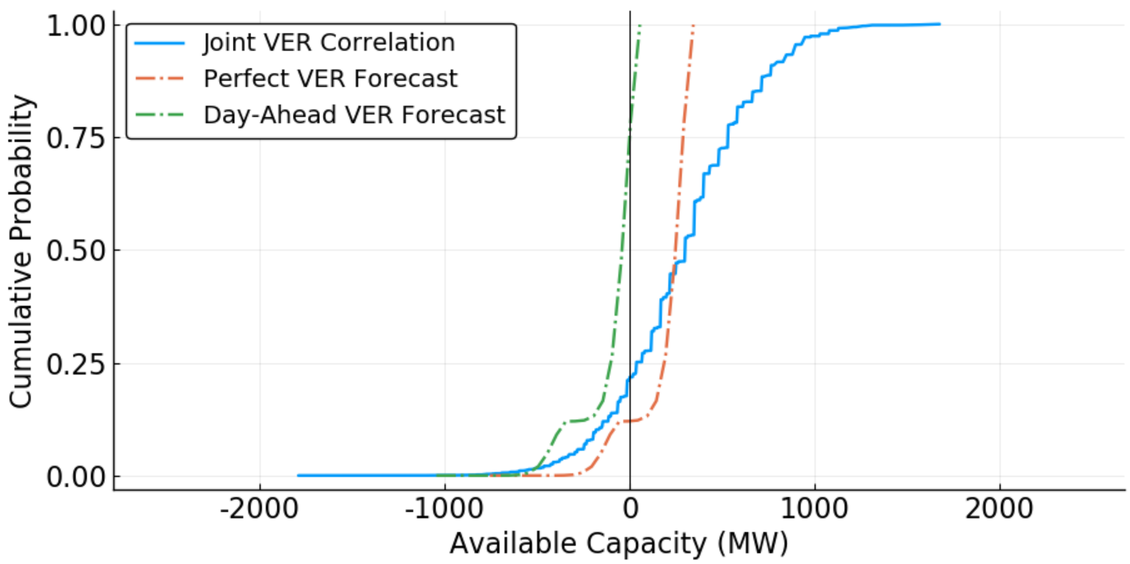

Figure 3.5: Loss of Load Probability snapshot during a July night from Region 3, Medium VER system. The 0MW axis crossing indicates the LOLP of each model distribution at the sampled t step.

Figures 3.6 and 3.7 highlight the differences between the Joint and Net VER models, particularly at the high VER penetration level. For the Low VER system cases, the Joint model curve exhibits similar skewness and kurtosis to the Net VER curves, and all LOLP distributions show 0% probability of load loss. However, at the High VER case, the curves have clearly shifted to a LOLP level that would be concerning to an operator. The Joint model shape also significantly changes, capturing the uncertainty of the increased amount of VER on the system. The Net VER models retain their shape and at the high VER level and mask the uncertainty of the wind and solar outputs.

Table 3.1: LOLE (in total annual hours) by region at low VER levels

	Region				
Capacity Model	**1**	**2**	**3**	**4**	**5**
Joint VER	38.622	26.298	21.543	20.710	20.619
Perfect Forecast	3.647	3.061	2.895	2.496	2.003
Day Ahead Forecast	5.770	8.744	8.574	6.023	6.277

Table 3.2: LOLE (in total annual hours) by region at medium VER levels

	Region				
Capacity Model	**1**	**2**	**3**	**4**	**5**
Joint VER	108.773	55.838	52.150	60.443	44.701
Perfect Forecast	12.493	7.160	6.526	4.481	2.443
Day Ahead Forecast	14.898	14.595	14.658	11.276	6.346

Table 3.3: LOLE (in total annual hours) by region at high VER levels

	Region				
Capacity Model	**1**	**2**	**3**	**4**	**5**
Joint VER	233.29	187.42	80.91	86.59	92.75
Perfect Forecast	59.03	66.70	12.23	7.06	11.79
Day Ahead Forecast	65.67	102.24	25.39	13.96	17.73

Although not considered a standard reliability metric, the "average per event EUE" $\frac{\text{EUE}}{\text{LOLEv}}$ was also calculated for each model. This metric captures the expected energy lost during any "event" seen by the model. An "event" is counted as any single hour with a non-zero loss of load probability. This is useful in comparing the magnitude of "events" seen by each model. As evidenced in Tables 3.4−3.6, in every regional case the Joint model captures a higher total energy (GWh) loss throughout the year of analysis. But the per event energy loss (Tables 3.7−3.9) in the day-ahead and perfect forecast models is higher than in the Joint model. This indicates that the relative risk captured by the net models poses more significant reliability risk than the loss events captured by the joint model. From an operator's perspective, the actions needed to mitigate the risk presented in these models is very different. The joint model indicates the need for more frequent, but small amounts of additional reserve generation; the net models indicate a less frequent need for additional reserves, but higher magnitude reserve requirements during higher risk event periods.

As [12] emphasizes, EUE can be used as a real-time indication of an oncoming high risk scenario. Given the rate at which VER can ramp, it's critical that an operator has adequate warning to position the system into a lower risk operating condition. The "net VER" approach to probabilistic modeling, even with perfect, real-time forecasts, fails to capture the characteristic uncertainty risk throughout the analysis. Because the "net VER" approach does not account for the spatially and temporally correlated uncertainty of the VER forecast, the characteristic shape of the probability curve tends to underestimate the loss of load likelihood. Further, an operator would be expected to take more significant action in response to the "net VER" curve approaching a loss of load scenario. The Joint model represents potentially more frequent, but lower magnitude need for spinning reserves.

Again, similar to [15], the increasing spatial diversity of VERs does smooth the output uncertainty in certain conditions (an example snapshot is shown in Figures A.6 and A.7). But there are diminishing returns on the correlation reduction; even in the largest regional spread of VER, the joint model shows statistically significant correlation between VER output which impacts the reliability metrics.

Table 3.4: EUE (in annual GWh) by region at low VER levels

	Region				
Capacity Model	**1**	**2**	**3**	**4**	**5**
Joint VER	11.931	6.870	5.057	4.798	5.015
Perfect Forecast	0.963	0.510	0.448	0.359	0.302
Day Ahead Forecast	1.331	1.403	1.455	0.845	0.890

Table 3.5: EUE (in annual GWh) by region at medium VER levels

	Region				
Capacity Model	**1**	**2**	**3**	**4**	**5**
Joint VER	66.988	25.689	20.628	25.843	17.522
Perfect Forecast	6.289	2.389	1.165	0.925	0.457
Day Ahead Forecast	7.038	4.844	3.647	2.543	1.005

Table 3.6: EUE (in annual GWh) by region at high VER levels

	Region				
Capacity Model	**1**	**2**	**3**	**4**	**5**
Joint VER	207.723	142.266	41.381	48.155	52.077
Perfect Forecast	35.800	30.397	3.037	1.931	2.678
Day Ahead Forecast	37.464	49.682	7.046	3.878	4.997

The statistical measures of skewness and kurtotis also provide insight into the characteristics of the probability distributions in each model. Results are shown in Tables 3.10−3.12. The high VER scenarios exhibit higher correlation, as evidenced by the lower kurtosis of the joint distribution relative to each regional system. This relates to intermittent generation patterns that are highly dependent on time and weather patterns. The low VER scenarios reduce the uncertainty of generation availability; this appears in the higher average kurtosis across all regions in the joint model. The opposite effect is seen in the Perfect Forecast and Day-Ahead forecast models because their probability distributions are determined solely by number of conventional generators in the system. This result is consistent with findings from [15] [28] [24], but uniquely includes multiple types of VER (wind and solar) with spatial and temporal correlations.

Tables 3.13 and 3.14 capture the variance of probability distribution shape for the joint capacity model at low, medium, and high VER levels. The skewness and kurtosis variance of the Perfect Forecast and Day-Ahead Forecast capacity models are zero in all instances, which is expected because the shape of both models is independent of the time-varying, correlated output distribution of VERs. No major trends appear from the variance tables, although this might be due to the conflation of factors from increased spatial diversity and VER levels, plus different compounding uncertainty from solar and wind resources. Generally, the High VER system model has higher variance in skewness and kurtosis in the smallest spatial region; the Low VER system model has higher kurtosis and skewness variance in the largest spatial region.

Table 3.7: Average EUE per Event (in MWh) by region at low VER levels

	Region				
Capacity Model	**1**	**2**	**3**	**4**	**5**
Joint VER	17.57	10.87	8.39	8.13	8.33
Perfect Forecast	11.88	4.72	3.59	2.90	2.72
Day Ahead Forecast	10.73	7.46	7.10	4.52	5.06

Table 3.8: Average EUE per Event (in MWh) by region at medium VER levels

	Region				
Capacity Model	**1**	**2**	**3**	**4**	**5**
Joint VER	64.66	32.60	28.22	35.45	27.08
Perfect Forecast	77.64	27.47	10.79	10.28	6.26
Day Ahead Forecast	75.68	40.70	23.53	19.27	9.85

Table 3.9: Average EUE per Event (in MWh) by region at high VER levels

	Region				
Capacity Model	**1**	**2**	**3**	**4**	**5**
Joint VER	118.02	90.10	46.34	55.16	56.61
Perfect Forecast	198.89	107.03	25.52	21.95	27.32
Day Ahead Forecast	179.25	133.20	40.50	30.53	35.95

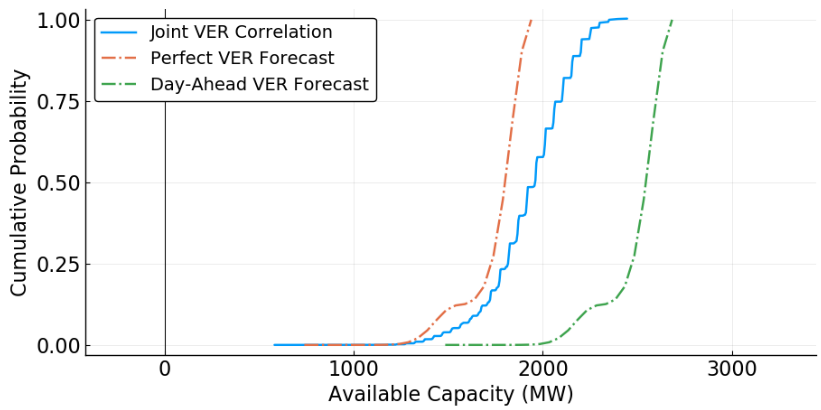

(a) Low VER, Region 3

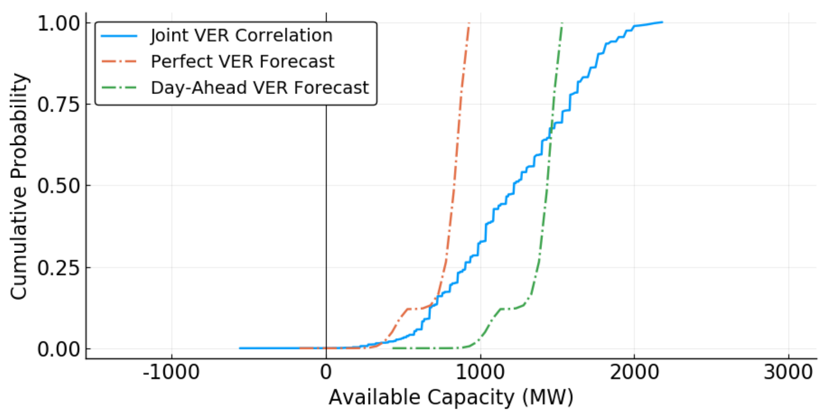

(b) Medium VER, Region 3

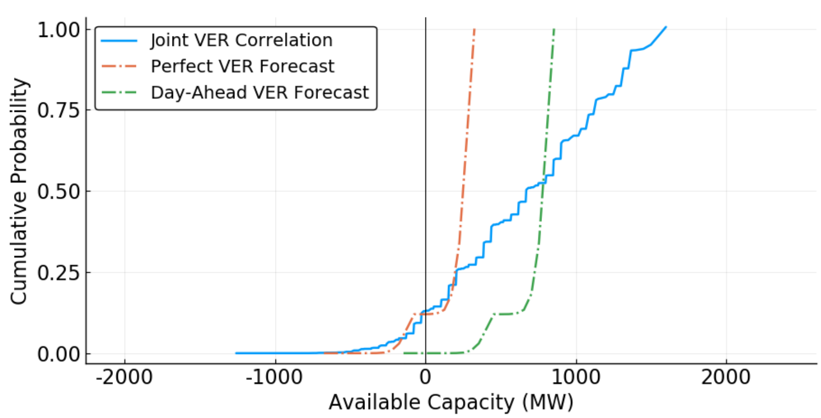

(c) High VER, Region 3

Figure 3.6: Loss of Load Probability snapshot during a July night from Region 3. The 0MW axis crossing indicates the LOLP of each model distribution at the sampled t step.

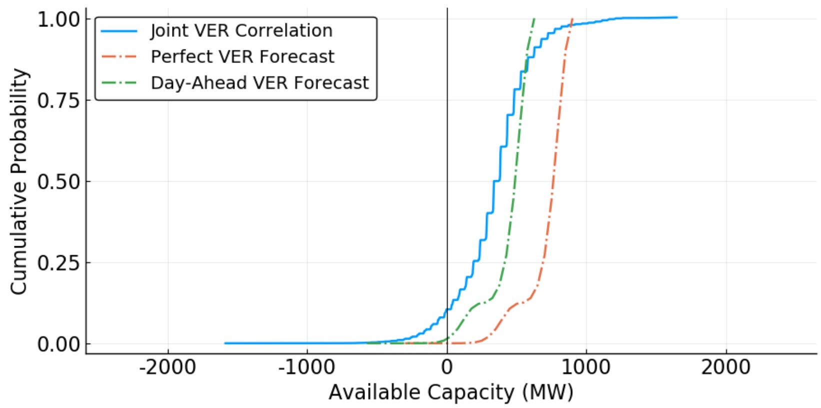

(a) Low VER, Region 5

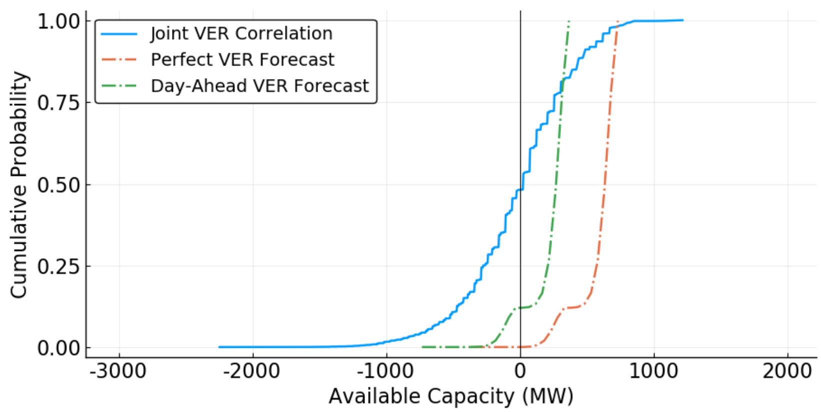

(b) Medium VER, Region 5

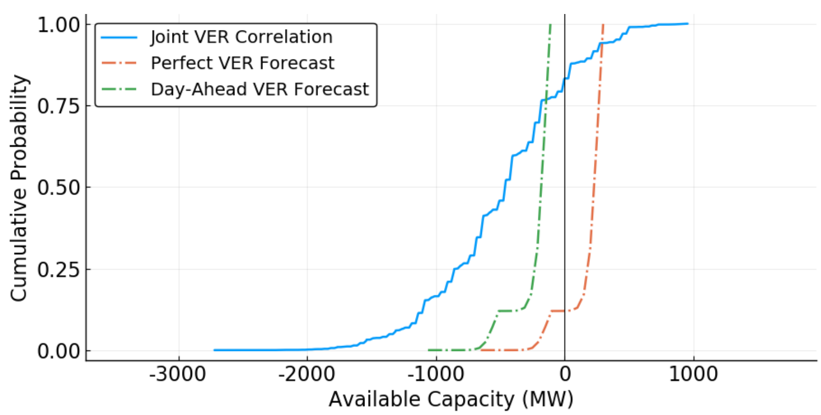

(c) High VER, Region 5

Figure 3.7: Loss of Load Probability distributions sample during a July evening from Region 5. The 0MW axis crossing indicates the LOLP of each model distribution at the sampled t step.

Table 3.10: Mean capacity distribution kurtosis by region at low VER levels

	Region				
Capacity Model	**1**	**2**	**3**	**4**	**5**
Joint VER	0.406	0.622	0.692	0.612	0.607
Perfect Forecast	2.027	2.027	2.027	2.036	2.036
Day Ahead Forecast	2.027	2.027	2.027	2.036	2.036

Table 3.11: Mean capacity distribution kurtosis by region at medium VER levels

	Region				
Capacity Model	**1**	**2**	**3**	**4**	**5**
Joint VER	0.124	0.081	0.270	0.202	0.227
Perfect Forecast	2.404	2.416	2.416	2.439	2.416
Day Ahead Forecast	2.404	2.416	2.416	2.439	2.416

Table 3.12: Mean capacity distribution kurtosis by region at high VER levels

	Region				
Capacity Model	**1**	**2**	**3**	**4**	**5**
Joint VER	0.303	0.113	0.242	0.125	0.155
Perfect Forecast	2.742	2.916	2.688	2.728	2.742
Day Ahead Forecast	2.742	2.916	2.688	2.728	2.742

Table 3.13: Joint Capacity Model kurtosis variance by region for all VER levels. The Net Models have zero variance in all instances.

	Region				
Joint Capacity Model	**1**	**2**	**3**	**4**	**5**
Low VER	0.288	0.436	0.610	0.548	0.506
Medium VER	0.410	0.196	0.319	0.277	0.311
High VER	0.983	0.247	0.385	0.274	0.249

Table 3.14: Joint Capacity Model skewness variance by region for all VER levels. The Net Models have zero variance in all instances.

	Region				
Joint Capacity Model	**1**	**2**	**3**	**4**	**5**
Low VER	0.165	0.134	0.199	0.158	0.176
Medium VER	0.166	0.133	0.116	0.094	0.097
High VER	0.257	0.170	0.207	0.126	0.090

Chapter 4
CONCLUSIONS AND RECOMMENDATIONS

4.1 Conclusions and Topics for Future Research

The purpose of this research was to investigate the influence of variable energy resource generation on the reliability analysis of power systems. It challenges the assumptions frequently applied in reliability analysis and advocates for more accurate representation of the generation characteristics of variable energy resources. In particular, it emphasizes the augmented reliability impact of dependencies between the variable generation resources. As seen in the results, if the influence of dependent output correlation from renewable energy sources is neglected, the loss of load probability under high penetrations of VER will be underestimated. It is critical that system operators understand the full implications of integrating highly uncertain energy resources into the grid. Further, this work highlights the value that uncertainty can play in reliability markets and ancillary services. Research into this topic, along with the impact of transmission constraints, will be critical in aiding the electric grid transition to 100% renewable resources.

4.1.1 Topics for Future Research

The following list of topics were simplified in the presented case study and should be explored in more detail:

- Load is assumed perfectly known with 100% probability of occurring. No day ahead load forecast is used and there is no conditional error or probabilistic outcome factored into subtracting load from the capacity availability model. Of course, load is not perfectly known and will follow a probabilistic curve much like the variable resources (and conventional resources). The impact of this load probability distribution should be explored in more detail. In particular, the spatial and temporal uncertainty correlations should be tied with the variable generator outputs.

- The load profile used here is taken exclusively from the GMLC data set which is spatially correlated with the southwest region of the United States. The spatial correlation study should be extended to adapt the load profile used in each “region” to better reflect a cumulative load profile of the area where the variable resources are being sourced from.

- The impact of transmission constraints, probability of sympathetic tripping, and cascading outages should be studied with a Monte Carlo model that incorporates the joint probability of VER availability.

- Load is assumed inelastic with no mechanism for demand response. Modeling demand response (including its appropriate probability model) in the loss of load probability is a topic for future research.

- The generic group of conventional generation sources is assumed to have the same availability. If Demand Response is considered part of that group (or some aggregated form of storage), it will likely have a more complex availability probability curve.

- The “Conventional” generation category includes battery storage and other energy limited resources. Those resources have state of charge management and energy capacity limitations that require various degrees of optimization and control to factor into decisions. Further research could characterize those factors into the joint capacity availability distribution.

- Consideration of Distributed Energy Resources: Arguably any resource on the distribution grid (Demand Response, rooftop solar, etc) do not belong in the capacity capability curve because they are not controlled by ISOs, NERC, bulk power system operators, etc. However, if they are not considered in the probabilistic calculation of the capacity availability curve, they should be accounted for as a contribution to the load "availability" curve (where Demand Response and rooftop solar have some likelihood of decreasing the load curve).

- The probability model trained here uses 1 year of data. A more comprehensive application of this method should ideally use at least 5 years of data to generate a more accurate model of the renewable output that takes better consideration of annually changing weather patterns and other influential factors [18].

- The Joint model could be compared with various independent VER models (similar to [5]) to further explore reliability metric model accuracy and evaluate potential trade-offs between computation time and accuracy of system representation.

BIBLIOGRAPHY

[1] Clayton Barrows, Aaron Bloom, Ali Ehlen, Jussi Ikaheimo, Jennie Jorgenson, Dheepak Krishnamurthy, Jessica Lau, Brendan McBennett, Matthew O'Connell, Eugene Preston, Andrea Staid, Gord Stephen, and Jean-Paul Watson. The IEEE Reliability Test System: A Proposed 2019 Update. *IEEE Transactions on Power Systems*, pages 1–1, jul 2019.

[2] Ricardo J. Bessa, Corinna Möhrlen, Vanessa Fundel, Malte Siefert, Jethro Browell, Sebastian Haglund El Gaidi, Bri Mathias Hodge, Umit Cali, and George Kariniotakis. Towards improved understanding of the applicability of uncertainty forecasts in the electric power industry. *Energies*, 10(9):1402, sep 2017.

[3] R. Billinton and A. A. Chowdhury. Incorporation of wind energy conversion systems in conventional generating capacity adequacy assessment. *IEE Proceedings C: Generation Transmission and Distribution*, 139(1):47–56, 1992.

[4] Roy Billinton and Ronald N. Allan. *Reliability Evaluation of Engineering Systems*. Springer US, Boston, MA, 1983.

[5] Carmen Lucia Tancredo Borges and Julio A.S. Dias. A Model to Represent Correlated Time Series in Reliability Evaluation by Non-Sequential Monte Carlo Simulation. *IEEE Transactions on Power Systems*, 32(2), 2017.

[6] ERCOT. ERCOT Market Information, 2020.

[7] Bethany Frew, Giulia Gallo, Gregory Brinkman, Michael Milligan, Kara Clark, and Aaron Bloom. Impact of Market Behavior, Fleet Composition, and Ancillary Services on Revenue Sufficiency. Technical report, National Renewable Energy Laboratory (NREL), Golden, CO (United States), jun 2016.

[8] Bri Mathias Hodge and Michael Milligan. Wind power forecasting error distributions over multiple timescales. In *IEEE Power and Energy Society General Meeting*, 2011.

[9] ISO-NE. About FCM Pay-for-Performance (PFP) Rules.

[10] ISO New England Inc. Energy Security Improvements ISO Discussion Paper. Technical report, ISO-NE, 2019.

[11] D. S. Kirschen, K. R W Bell, D. P. Nedic, D. Jayaweera, and R. N. Allan. Computing the value of security. *IEE Proceedings: Generation, Transmission and Distribution*, 150(6):673–678, nov 2003.

[12] Daniel S. Kirschen, Dilan Jayaweera, Dusko P. Nedic, and Ron N. Allan. A probabilistic indicator of system stress. *IEEE Transactions on Power Systems*, 19(3):1650–1657, aug 2004.

[13] Daniel Sadi Kirschen. *Fundamentals of power system economics.* Wiley, Hoboken, second edition. edition, 2019.

[14] D. Lew, G. Brinkman, E. Ibanez, B. M. Hodge, M. Hummon, A. Florita, and M. Heaney. The Western Wind and Solar Integration Study Phase 2. Technical report, National Renewable Energy Laboratory (NREL), Golden, CO (United States), sep 2013.

[15] Henry Louie. Correlation and statistical characteristics of aggregate wind power in large transcontinental systems. *Wind Energy*, 17(6):793–810, jun 2014.

[16] Henry Louie. Evaluation of bivariate Archimedean and elliptical copulas to model wind power dependency structures. *Wind Energy*, 17(2):225–240, feb 2014.

[17] Michael Milligan. Resource Adequacy: Connecting Existing Methods, Tools, and Metrics with the Future Grid, 2020.

[18] Michael Milligan, Bethany Frew, Eduardo Ibanez, Juha Kiviluoma, Hannele Holttinen, and Lennart Söder. Capacity value assessments of wind power, jan 2017.

[19] MISO. Automatic Generation Control (AGC) Enhancement for Fast-Ramping Resources.

[20] Roger B. Nelsen. *An introduction to Copulas (Springer Series in Statistics)*. 2006.

[21] IVGTF NERC. NERC IVGTF Task 1-6: Probabilistic Methods. Technical report, NERC, 2014.

[22] NERC IVGTF Subcommittee. ”Integration of Variable Generation Task Force Probabilistic Techniques”. Technical report, NERC, 2011.

[23] NREL. Probabilistic Resource Adequacy Suite (PRAS), 2020.

[24] Edgar Nuño Martinez, Nicolaos Cutululis, and Poul Sørensen. High dimensional dependence in power systems: A review. *Renewable and Sustainable Energy Reviews*, 94:197–213, oct 2018.

[25] Office of Electric Reliability and Enforecement. NERC - Summer 2019 Reliability and Energy Market Assessment. Technical report, NERC, 2019.

[26] G. Papaefthymiou. *Integration of stochastic generation in power systems*. PhD thesis, 2005.

[27] George Papaefthymiou and Dorota Kurowicka. Using copulas for modeling stochastic dependence in power system uncertainty analysis. *IEEE Transactions on Power Systems*, 24(1):40–49, 2009.

[28] George Papaefthymiou and Pierre Pinson. Modeling of Spatial Dependence in Wind Power Forecast Uncertainty. In *Proceedings of the 10th International Conference on Probablistic Methods Applied to Power Systems*, Rincon, 2008. IEEE.

[29] Phil Pettingill, Julia Matevosyan, Erik Ela, and Jessica Harrison. Session 5: Market Design Evolution for High Share of Renewables, 2020.

[30] Pierre Pinson. *Estimation of the uncertainty in wind power forecasting*. PhD thesis, 2006.

[31] Pierre Pinson, Christophe Chevallier, and George N. Kariniotakis. Trading wind generation from short-term probabilistic forecasts of wind power. *IEEE Transactions on Power Systems*, 22(3):1148–1156, aug 2007.

[32] Eugene Preston and Clayton Barrows. Evaluation of year 2020 IEEE RTS generation reliability indices. In *2018 International Conference on Probabilistic Methods Applied to Power Systems, PMAPS 2018 - Proceedings*. Institute of Electrical and Electronics Engineers Inc., Aug 2018.

[33] Yan G. Rebours, Daniel S. Kirschen, Marc Trotignon, and Sébastien Rossignol. A survey of frequency and voltage control ancillary services - Part II: Economic features. *IEEE Transactions on Power Systems*, 22(1):358–366, feb 2007.

[34] Julija Tastu, Pierre Pinson, and Henrik Madsen. Multivariate conditional parametric models for a spatio-temporal analysis of short-term wind power forecast errors. Technical report, Technical University of Denmark, 2010.

[35] Charles W. Therrien and Murali Tummala. *Probability and random processes for electrical and computer engineers*. CRC Press, 2 edition, jan 2012.

[36] Egill Tomasson and Lennart Soder. Generation Adequacy Analysis of Multi-Area Power Systems with a High Share of Wind Power. *IEEE Transactions on Power Systems*, 33(4):3854–3862, jul 2018.

[37] UCLA Luskin Center for Innovation. 100% Clean Energy Progress Report. Technical report, UCLA, nov 2019.

[38] U.S. Energy Information Administration. Electricity data browser - Net generation for electric power, 2019.

[39] M. Vaiman, K. Bell, Y. Chen, B. Chowdhury, I. Dobson, P. Hines, M. Papic, S. Miller, and P. Zhang. Risk assessment of cascading outages: Methodologies and challenges. *IEEE Transactions on Power Systems*, 27(2):631–641, may 2012.

[40] Yih Huei Wan, Michael Milligan, and Brian Parsons. Output power correlation between adjacent wind power plants. *Journal of Solar Energy Engineering, Transactions of the ASME*, 125(4):551–555, nov 2003.

[41] Yi Wang, Ning Zhang, Chongqing Kang, Miao Miao, Rui Shi, and Qing Xia. An Efficient Approach to Power System Uncertainty Analysis With High-Dimensional Dependencies. *IEEE Transactions on Power Systems*, 33(3):2984–2994, may 2018.

[42] Ning Zhang, Chongqing Kang, Chanan Singh, and Qing Xia. Copula Based Dependent Discrete Convolution for Power System Uncertainty Analysis. *IEEE Transactions on Power Systems*, 31(6):5204–5205, nov 2016.

Appendix A

EXTENDED RESULTS

Extended results from 3.1

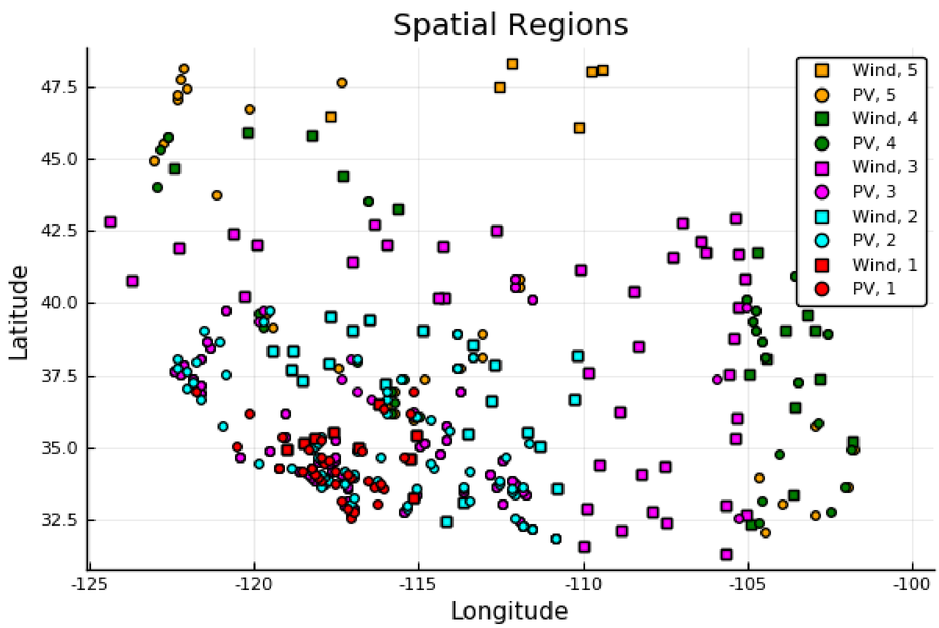

Figure A.1: Regions used for Spatial Correlation study. Colors indicate subsets of increasingly larger regions.

Tables of installed capacity by resource type used for each test scenario. Values vary slightly by scenario due to the discrete number and capacities of VER sites in the historical data set. The "other dispatchable" category is adjusted per scenario to maintain a constant total effective load carrying capacity for the system.

Table A.1: Low VER scenario - generation resource nameplate capacity (in GW) by region.

Nameplate Capacity (GW) by region					
Resource	**1**	**2**	**3**	**4**	**5**
Wind	4.19	4.29	4.27	4.22	4.35
Solar	4.04	4.01	3.93	4.29	4.10
Other Dispatchable	5.85	5.85	5.85	5.80	5.80
Total	**14.08**	**14.15**	**14.05**	**14.30**	**14.25**

Table A.2: Medium VER scenario - generation resource nameplate capacity (in GW) by region.

Nameplate Capacity (GW) by region					
Resource	**1**	**2**	**3**	**4**	**5**
Wind	8.51	8.15	8.21	8.02	8.18
Solar	7.63	7.95	7.85	8.29	7.88
Other Dispatchable	3.95	3.90	3.90	3.80	3.90
Total	**20.10**	**19.99**	**19.95**	**20.11**	**19.96**

Table A.3: High VER scenario - generation resource nameplate capacity (in GW) by region.

Nameplate Capacity (GW) by region					
Resource	**1**	**2**	**3**	**4**	**5**
Wind	10.49	11.22	10.43	10.36	10.20
Solar	10.73	11.98	10.07	10.48	10.81
Other Dispatchable	2.60	2.00	2.80	2.65	2.60
Total	**23.81**	**25.21**	**23.30**	**23.48**	**23.61**

The following samples show detailed Joint distributions and Marginal distributions from a selection of time stamps in the system data. The stacked bar chart represents actual power production (in MW) at the time shown; the legend in the stacked bar shows installed capacity of conventional generation, and total installed ELCC of Wind and Solar.

Table A.4: Mean capacity distribution skewness by region at low VER levels

	Region				
Capacity Model	**1**	**2**	**3**	**4**	**5**
Joint VER	-0.236	-0.233	-0.318	-0.266	-0.293
Perfect Forecast	-1.626	-1.626	-1.626	-1.631	-1.631
Day Ahead Forecast	-1.626	-1.626	-1.626	-1.631	-1.631

Table A.5: Mean capacity distribution skewness by region at medium VER levels

	Region				
Capacity Model	**1**	**2**	**3**	**4**	**5**
Joint VER	-0.143	-0.167	-0.155	-0.189	-0.196
Perfect Forecast	-1.824	-1.829	-1.829	-1.841	-1.829
Day Ahead Forecast	-1.824	-1.829	-1.829	-1.841	-1.829

Table A.6: Mean capacity distribution skewness by region at high VER levels

	Region				
Capacity Model	**1**	**2**	**3**	**4**	**5**
Joint VER	-0.196	-0.100	-0.208	-0.153	-0.177
Perfect Forecast	-1.993	-2.077	-1.966	-1.986	-1.993
Day Ahead Forecast	-1.993	-2.077	-1.966	-1.986	-1.993

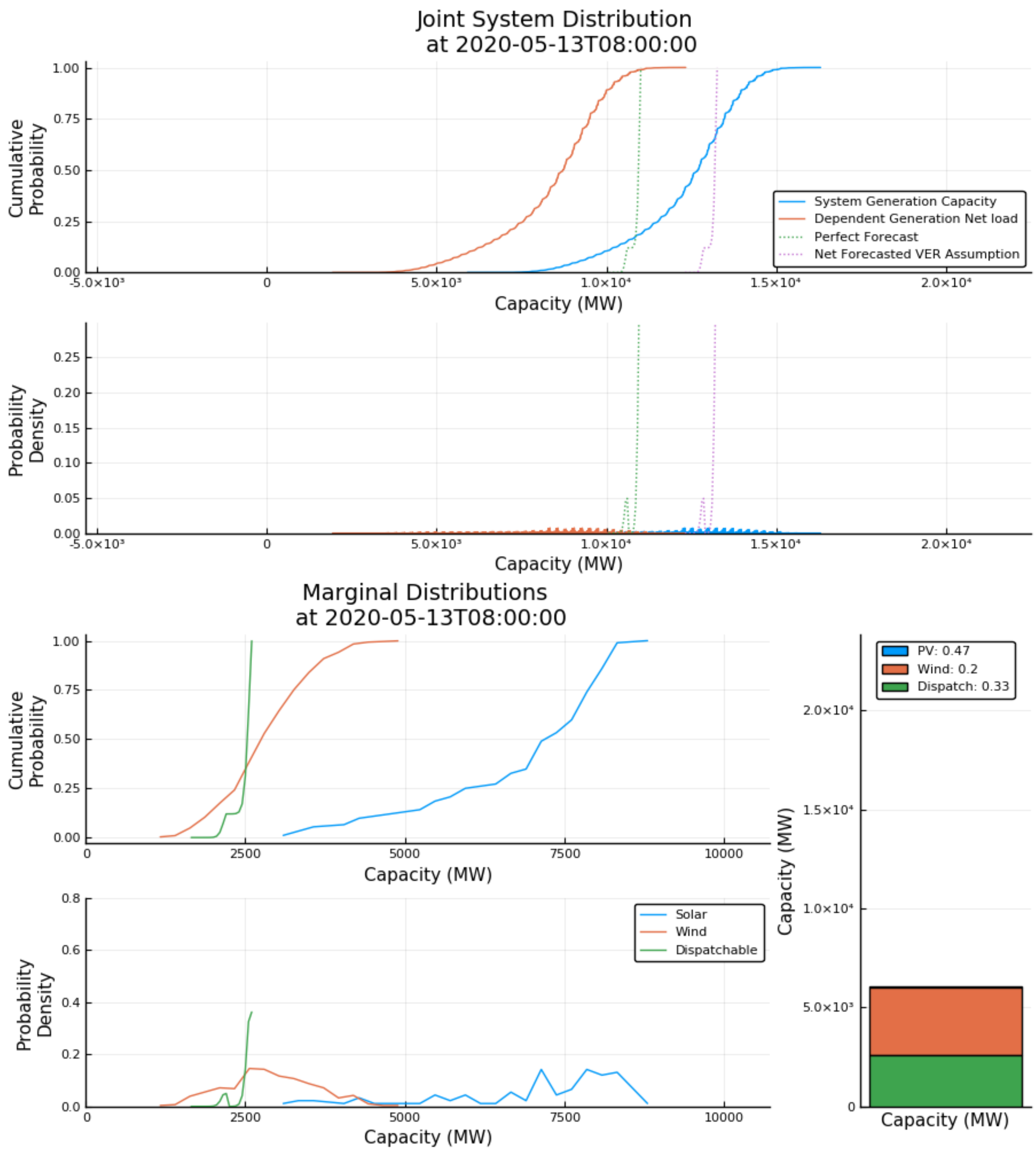

Figure A.2: Scenario summary from Region 1, high VER, spring morning

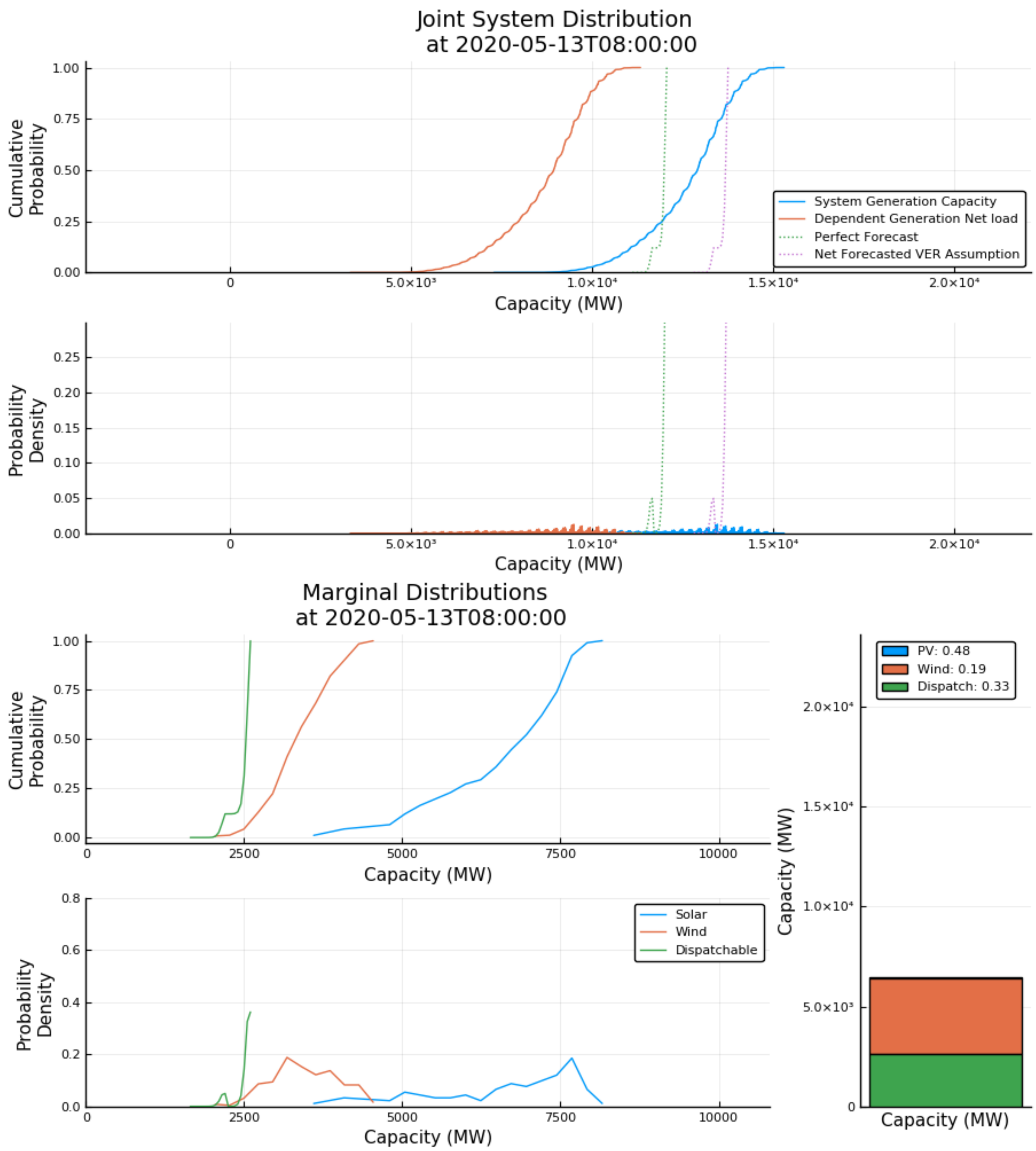

Figure A.3: Scenario summary from Region 5, high VER, spring morning

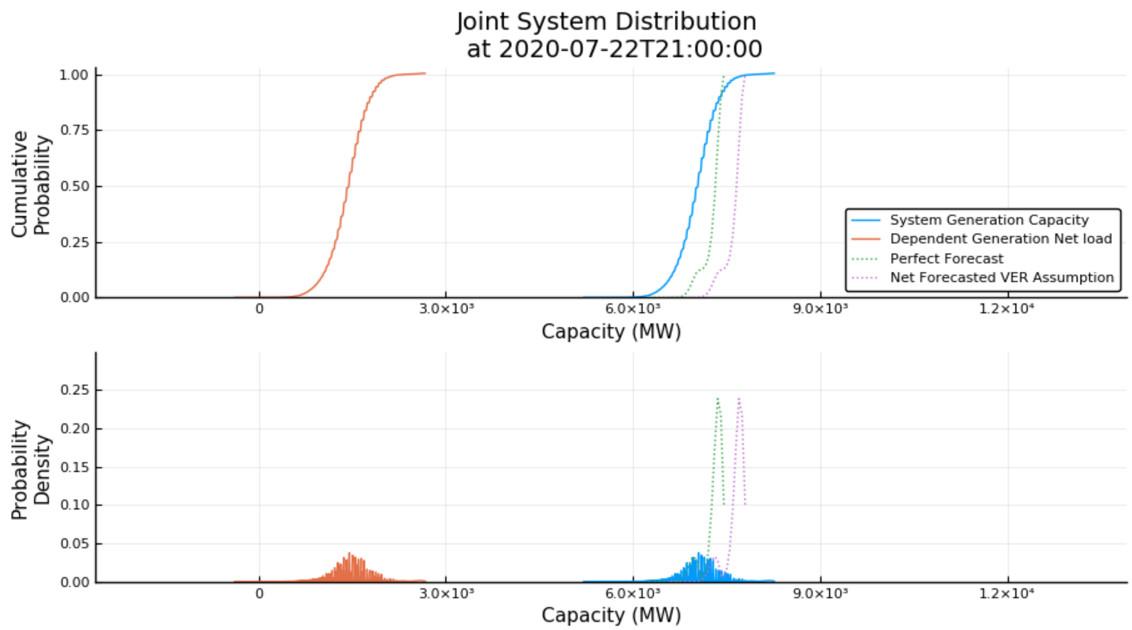

Figure A.4: Capacity Availability model sample from Region 1, low VER, summer late evening

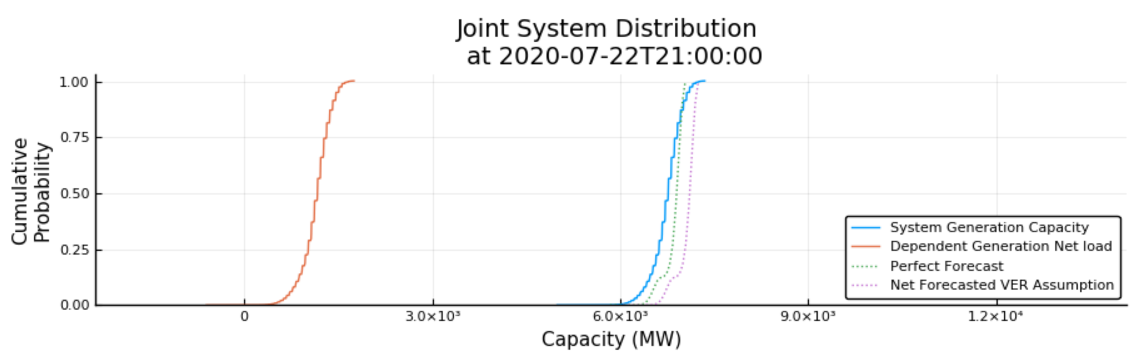

Figure A.5: Capacity Availability model sample from Region 5, low VER, summer late evening

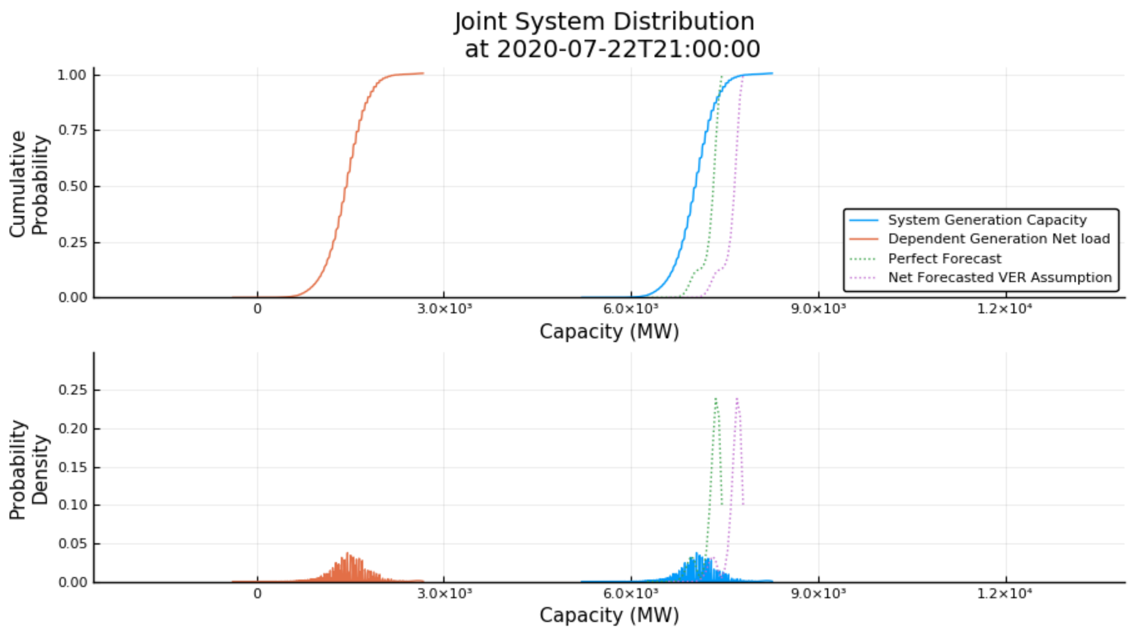

Figure A.6: Capacity Availability model sample from Region 1, high VER, summer late evening

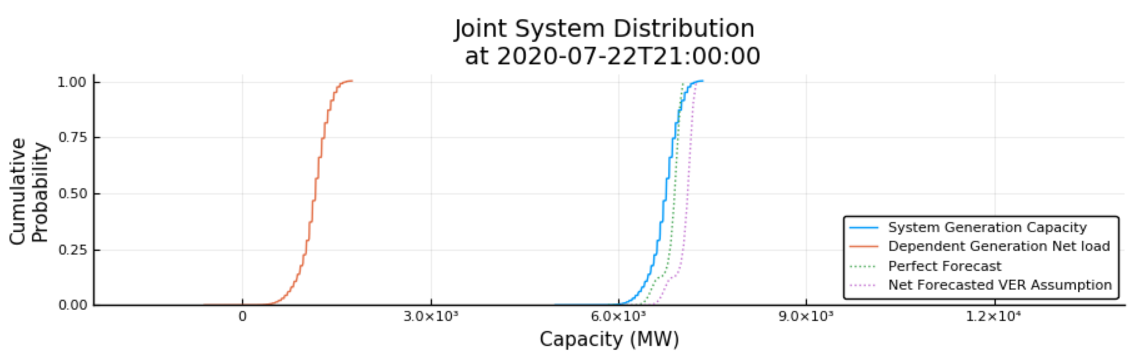

Figure A.7: Capacity Availability model sample from Region 5, high VER, summer late evening

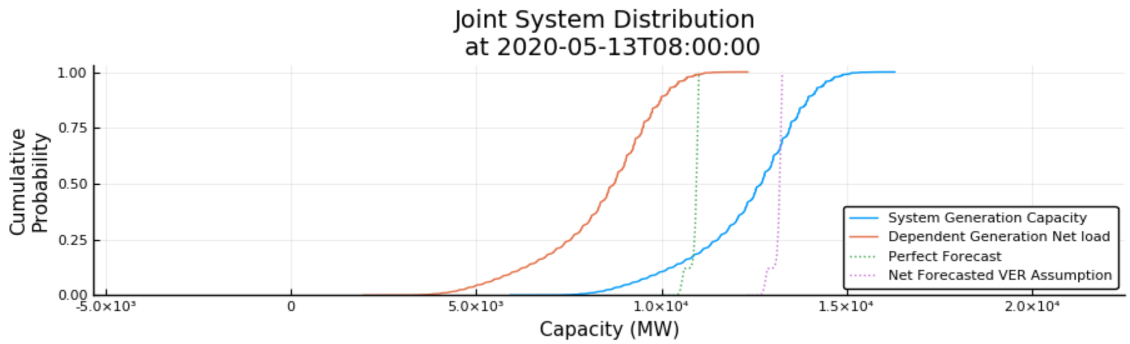

Figure A.8: Scenario summary from Region 1, high VER, spring morning

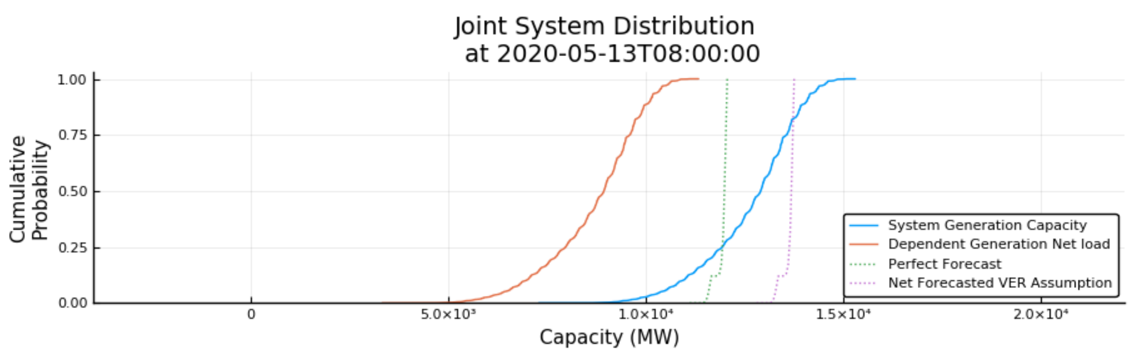

Figure A.9: Scenario summary from Region 5, high VER, spring morning